

SD-TR-83-53

**Stress-Corrosion Crack-Growth  
Study of Titanium Alloy  
Ti-6Al-4V Exposed to  
Freon PCA and Nitrogen  
Tetroxide MON-1**

**R. A. Bjorklund**

**August 1, 1983**

**Prepared for  
Air Force Headquarters Space Division  
through an agreement with  
National Aeronautics and Space Administration  
by  
Jet Propulsion Laboratory  
California Institute of Technology  
Pasadena, California**

**JPL PUBLICATION 83-31**

The research described in this publication was carried out by the Jet Propulsion Laboratory, California Institute of Technology, and was sponsored by the Air Force Headquarters Space Division through an agreement with NASA. Reference to any specific commercial product, process, or service by trade name or manufacturer does not necessarily constitute an endorsement by the United States Government or the Jet Propulsion Laboratory, California Institute of Technology.

## NOTICES


When U.S. Government drawings, specifications, or other data are used for any purpose other than a definitely related government procurement operation, the Government thereby incurs no responsibility nor any obligation whatsoever, and the fact that the Government may have formulated, furnished, or in any way supplied the said drawings, specifications, or other data is not to be regarded by implication or otherwise, or in any manner, as licensing the holder or any other person or corporation, or conveying any rights or permission to manufacture, use, or sell any patented invention that may in any way be related thereto.


## FOREWORD

The work reported herein was sponsored by the Air Force Headquarters Space Division, Air Force Systems Command, Los Angeles, California, under military Interdepartmental Purchase Request, Project Order Number FY 7616-81-0-0354. The program was administered under the Technical Direction of Major James Anthony and Captain Scott Wymore, Propulsion Systems, SD/YRE.

The work was carried out by the Jet Propulsion Laboratory of the California Institute of Technology, under NASA Task Order Number RE-182, Amendment Number 131, under NASA Contract Number NAS7-918.

The Space Division Public Affairs Office has reviewed the report and determined that it is releasable to the National Technical Information Service, where it will be available to the general public, including foreign nationals. This technical report is approved for release and distribution in accordance with the distribution statement on the cover and on the DD Form 1473.

  
James Anthony, Major, USAF  
Chief, Propulsion System  
Project Manager

  
David Richardson, Colonel USAF  
Program Director, Satellite  
Data System Office

REPORT DOCUMENTATION PAGE		READ INSTRUCTIONS BEFORE COMPLETING FORM
1. REPORT NUMBER SD-TR-83-53	2. GOVT ACCESSION NO.	3. RECIPIENT'S CATALOG NUMBER
4. TITLE (and Subtitle) Stress-Corrosion Crack-Growth Study of Titanium Alloy Ti-6Al-4V Exposed to Freon PCA and Nitrogen Tetroxide MON-1	7. AUTHOR(s)  Roy A. Bjorklund	5. TYPE OF REPORT & PERIOD COVERED Final February 1981 to March 1983
		6. PERFORMING ORG. REPORT NUMBER JPL 83-31
9. PERFORMING ORGANIZATION NAME AND ADDRESS Jet Propulsion Laboratory 4800 Oak Grove Drive Pasadena, California 91109	11. CONTROLLING OFFICE NAME AND ADDRESS Air Force Headquarters Space Division Air Force Systems Command Los Angeles, California 90009	8. CONTRACT OR GRANT NUMBER(s)  FY7616-81-0-0354
		10. PROGRAM ELEMENT, PROJECT, TASK AREA & WORK UNIT NUMBERS
14. MONITORING AGENCY NAME & ADDRESS (if different from Controlling Office)	12. REPORT DATE August 1983	13. NUMBER OF PAGES 64
		15. SECURITY CLASS. (of this report) Unclassified
16. DISTRIBUTION STATEMENT (of this Report)  Approved for public release. Distribution unlimited.	17. DISTRIBUTION STATEMENT (of the abstract entered in Block 20, if different from Report)	15a. DECLASSIFICATION/DOWNGRADING SCHEDULE N/A
		18. SUPPLEMENTARY NOTES  Technical work accomplished through an agreement with the National Aeronautics and Space Administration
19. KEY WORDS (Continue on reverse side if necessary and identify by block number)	Stress-corrosion cracking Nitrogen tetroxide MON-1 Fracture mechanics Propellant/Material Compatibility Titanium Alloy Ti-6Al-4V Satellite Propellant Tanks Freon, Precision Cleaning Agent	
20. ABSTRACT (Continue on reverse side if necessary and identify by block number) An experimental fracture-mechanics program was performed to determine the stress-corrosion crack-growth sensitivity of the propellant tank material, titanium alloy Ti-6Al-4V, for aerospace satellite applications involving long-term exposure to Freon PCA and nitrogen tetroxide MON-1. Sustained-load tests were made at a 49°C (120°F) constant temperature using thin-gauge tensile test specimens containing semielliptical surface flaws. Test specimen types included parent metal, center of weld, and weld-heat-affected zone. It was		

concluded that Ti-6Al-4V alloy is not adversely affected in a stress environment when exposed to Freon PCA for 1000 hours followed by exposure to nitrogen tetroxide MON-1 for 2000 hours at stress levels up to 80% of the experimental critical plane-strain stress-intensity factor.

**UNCLASSIFIED**

**SECURITY CLASSIFICATION OF THIS PAGE (When Data Entered)**

# CONTENTS

I.	INTRODUCTION -----	6
A.	Background Information -----	6
B.	Program Objective -----	8
C.	Description of Work -----	8
D.	Scope of Program -----	9
E.	Method of Qualification -----	10
II.	SOLVENT/PROPELLANT AND MATERIAL -----	11
A.	Solvent/Propellant Procurement -----	11
B.	Solvent/Propellant Characterization -----	11
C.	Material Procurement -----	13
D.	Material Characterization -----	13
III.	TEST PROGRAM -----	18
A.	Test Procedure -----	18
B.	Test Specimen Preparation -----	19
C.	Testing -----	28
D.	Posttest -----	35
IV.	RESULTS -----	38
A.	Summary -----	38
B.	Inert Fracture Tests -----	38
C.	Stress-Corrosion Crack-Growth Tests -----	41
D.	Dimpling -----	45
E.	Scanning Electron Microscopy -----	46
V.	CONCLUSIONS -----	53

VI. RECOMMENDATIONS -----	54
DEFINITION OF TERMS -----	55
REFERENCES -----	58
APPENDIX A. LINEAR-ELASTIC FRACTURE MECHANICS -----	59

### Tables

1. Nitrogen Tetroxide MON-1 Analyses -----	12
2. Test Matrix -----	20
3. Pretest Cracking and Posttest Marking of JPL Test Specimens -----	21
4. Pretest Cracking and Posttest Marking of AFSD Test Specimens -----	26
5. Inert Fracture Test Data for JPL Test Specimens -----	39
6. Inert Fracture Test Data for AFSD Test Specimens -----	40
7. Average Values of $K_{Ie}$ for AFSD Test Specimens -----	41
8. Nominal Sustained-Load Flaw-Growth Test Data for JPL Specimens -----	43
9. Nominal Sustained-Load Flaw-Growth Test Data for AFSD Specimens -----	43
10. Maximum Sustained-Load Flaw-Growth Test Data for AFSD Specimens -----	44
11. AFSD Specimen Backface Dimple Stresses -----	45

### Figures

1. Satellite Data Systems Satellite Liquid-Propulsion System -----	7
2. Satellite Data Systems Liquid-Propellant Tank -----	7
3. Typical AFSD Weldment Test Specimen -----	14
4. Typical HAC Propellant Tank Weldment Section -----	17

5.	Typical AFSD Test Specimen Weldment Section -----	17
6.	AFSD Test Specimen With EDM Starter Notch -----	23
7.	Typical Starter Notches in Three Types of AFSD Test Specimens -----	24
8.	Instron Model 1331 Servo-Hydraulic Test System with Beam-Bending Fixture -----	25
9.	MTS Systems Corporation Crack-Opening-Displacement-Type Extensometer Installed on Liquid-Nitrogen Inert Fracture Test Specimen -----	25
10.	MTS Systems Corporation Model 810 Servo-Hydraulic Testing System with Environmental Chamber -----	29
11.	Typical Stress/Strain Curves for Parent-Metal-Specimen Inert Fracture Tests -----	30
12.	Typical Stress/Strain Curves for Center-Weld-Specimen Inert Fracture Tests -----	31
13.	Typical Stress/Strain Curves for Heat-Affected-Zone-Specimen Inert Fracture Tests -----	32
14.	Propellant-Cup Test Fixture -----	33
15.	Propellant-Cup Installed on Typical Test Specimen -----	33
16.	Stress-Level Profiles for Tank Leak Check and Proof Test ----	34
17.	Satec Systems Incorporated Model C Static-Load Testing Machine Facility -----	36
18.	Typical Installation of Two Sustained-Load Test Specimens in Series -----	36
19.	Typical Example of Posttest Backface Dimple from Sustained-Load Testing -----	46
20.	Parent-Metal Specimen AFSD-14-P After Sustained-Load- Testing Exposure to Freon PCA and NTO MON-1 -----	47
21.	Center-Weld Specimen AFSD-11-C After Sustained-Load- Testing Exposure to Freon PCA and NTO MON-1 -----	48
22.	Weld-Heat-Affected-Zone Specimen AFSD-11-H After Sustained-Load-Testing Exposure to Freon PCA and NTO MON-1 --	49
23.	Control Specimen AFSD-4-H After Sustained-Load- Testing Exposure to Freon PCA and GN <sub>2</sub> -----	50



24.	Control Specimen AFSD-14-H After Sustained-Load- Testing Exposure to Air Only -----	51
25.	Cross Section of Lateral Fracture in Backface Dimple of AFSD-5-C Specimen -----	52
A-1.	Shape Parameter Curves for Surface Flaws -----	60
A-2.	Magnification Factor Curves -----	60

## ACKNOWLEDGEMENT

This investigation was performed by the Jet Propulsion Laboratory under the technical cognizance of the Propulsion Systems Section, Control and Energy Conversion Division.

Many people contributed to the success of the program reported herein. The author would like to acknowledge the assistance and contributions of the following:

### Advanced Technology and Applications

Dr. M. Dowdy  
Mrs. K. Moran

### Edwards Test Station

Mr. R. Maciel  
Mr. J. Short  
Mr. C. Worthen

### Analytical Chemistry Laboratory

Mr. R. Haack  
Mr. C. Moran  
Ms. L. Taylor

### Applied Mechanics Technology

Dr. E. Chow  
Mr. T. Hill

### Scanning Electron Microscopy

Mr. J. Collier

### Fabrication

Mr. H. Ferguson

### Documentation

Dr. M. F. Buehler  
Mr. D. Fulton

### Aerospace Corporation

Mr. S. Frederick  
Mr. C. Martinez

### Hughes Aircraft Company

Mr. F. Anderson  
Mr. W. Butcher

## SECTION I

### INTRODUCTION

#### A. BACKGROUND INFORMATION

The U.S. Air Force Headquarters Space Division (AFSD) is actively supporting the design and development of the new Satellite Data Systems (SDS) Satellite to be placed in orbit using the Space Transportation System (STS). A summary of the propulsion subsystem for the SDS Satellite is given in Ref. 1. The spacecraft is designed to take advantage of the Space Shuttle's large cargo bay and payload capability. The concept is based upon Hughes Aircraft Company's spin-stabilized SYNCON IV Spacecraft, which was later upgraded and employed on LEASAT. It is a 4.3- to 4.6-m- (14- to 15-ft-) diameter spacecraft with a hybrid liquid/solid rocket propulsion system; it is shown in Fig. 1. Upon ejection from the STS, the solid motor is used to place the spacecraft into a low Earth orbit; the liquid-bipropellant thrusters are used for trajectory correction and attitude control, including spin-up.

The SDS liquid-propulsion system contains eight identical conispherical propellant tanks; four contain monomethylhydrazine (MMH) fuel and four contain nitrogen tetroxide (NTO) with mixed oxides of nitrogen number one (MON-1). Each tank is 838 mm (33 in.) in diameter, and weighs 16.1 kg (35.6 lb). The tanks are fabricated from a titanium alloy of 90 titanium, six aluminum, and four vanadium proportions (Ti-6Al-4V) by Fansteel, Precision Sheet Metal, Los Angeles, California. A drawing of one of these tanks is shown in Fig. 2. Tank volume is 0.317 m<sup>3</sup> (19,350 in.<sup>3</sup>); the tank will operate at 1792 kPa (260 psig), and has a burst pressure of 3584 kPa (520 psig). The gas-pressurization inlet is on the hemispherical end, and the propellant outlet is on the cone-shaped end. The propellant outlet is oriented toward the outer perimeter of the spinning spacecraft, eliminating the need for a positive expulsion device.

In the manufacturing and qualification of these tanks, those designated for MMH fuel are cleaned, leak-checked, proof-tested, and expulsion-tested using isopropyl alcohol (IPA) as the solvent and referee fluid. In the same manner, Freon Precision Cleaning Agent (PCA) is used in the tanks designated for NTO MON-1 oxidizer service. It is well-known that IPA contamination of MMH will not induce stress-corrosion cracking or hydrogen embrittlement in Ti-6Al-4V alloy tanks, whereas Freon-solvent contamination of hydrazine derivative fuels will (Ref. 2). There was no conclusive documentation that Freon PCA contamination of NTO MON-1 would not induce similar stress-corrosion cracking or embrittlement in Ti-6Al-4V alloy tanks. Therefore, a fracture-mechanics program was needed to evaluate this potential solvent/propellant/material compatibility problem.

Satellite requirements for SDS include a 10-yr mission life, which places it in the category of such NASA deep-space probes as the Mariner, Viking, and Voyager spacecraft. Long-term (10-yr or more) propellant/material compatibility has been an on-going program at the Jet Propulsion

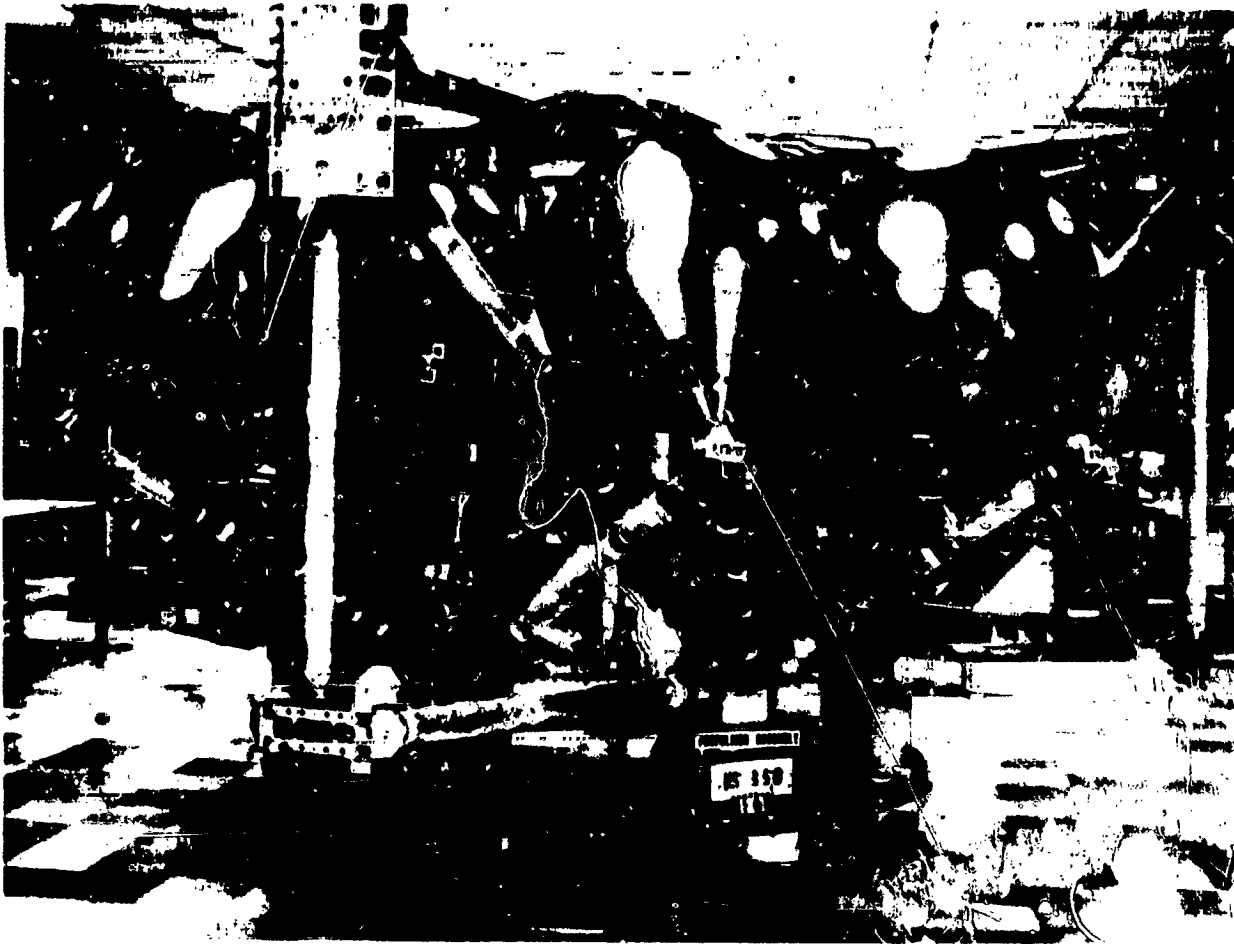
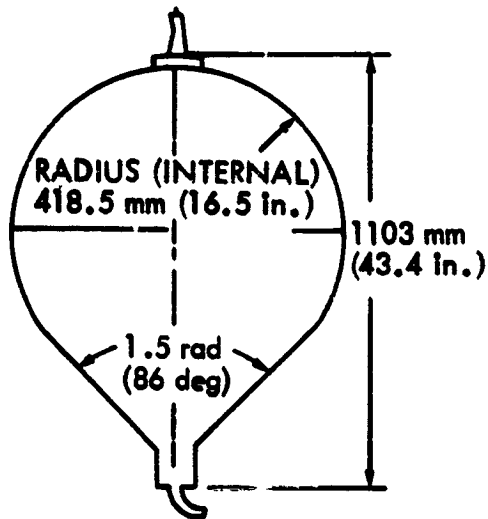


Figure 1. Satellite Data Systems Satellite Liquid-Propulsion System  
(Courtesy of Hughes Aircraft Company)



MANUFACTURER: FANSTEEL

PRESSURE RANGES:

OPERATING 1792 kPa (260 psig)

PROOF 2826 kPa (410 psig) est

BURST 3584 kPa (520 psig)

TEMPERATURE RANGE: 12 TO 77°C (10 TO 170°F)

VOLUME: 317 m<sup>3</sup> (19,341 in.<sup>3</sup>)

WEIGHT: 16.1 kg (35.6 lbm)

MATERIAL: Ti-6Al-4V

Figure 2. Satellite Data Systems Liquid-Propellant Tank (Ref. 1)

Laboratory (JPL) since 1968. Unique facilities and capabilities have been developed to conduct real-time experiments involving the contact of inert materials with Earth-storable propellants. The facilities' capabilities include controlled environment storage of hermetically sealed glass capsules containing propellant/material specimens, and machines for sustained-load testing of material with exposure to propellants. The information obtained from this type of testing has been used in the design of propellant systems for past, present, and future spacecraft.

AFSD sponsored this fracture-mechanics program at JPL to evaluate a possible stress-corrosion cracking problem for SDS involving Freon PCA, NTO MON-1, and Ti-6Al-4V alloy. However, the same information will be very useful to the forthcoming NASA Galileo Spacecraft, which will use the same combination of solvent, propellant, and material.

## B. PROGRAM OBJECTIVE

The objective of this program is to experimentally determine if the use of Freon PCA (as a cleaning solvent and referee test fluid) in series with NTO MON-1 will cause stress-corrosion crack growth in Ti-6Al-4V propellant tank material.

## C. DESCRIPTION OF WORK

The experimental test program used standard tensile test specimens provided by both JPL and AFSD. Existing specimens from two previous JPL programs, Mariner 1971 and Viking Orbiter 1975, were used initially to determine preliminary results as quickly as possible to satisfy the immediate needs of the AFSD space satellite tank production program. AFSD specimens supplied later were made using the same heat of titanium forgings and manufacturing processes used by Fansteel to manufacture the propellant tanks for Hughes Aircraft Company (HAC). The manufacturing processes used were identical for all specimens and included annealing, rough machining, solution heat treatment and aging, finish machining, cleaning, welding, radiographic inspection, penetrant inspection, vacuum aging, and final machining to specimen size. Only one type of specimen, a weldment, was made. It had the same thickness as the propellant tank weld joint it represented. Specimens were prepared for testing with semielliptical surface flaws (precracking) of one nominal size. The selected location of the flaw determined the type of fracture-mechanics specimen to be tested as either a parent metal (P), center of weld (C), or weld-heat-affected zone (H).

Inert fracture tests were conducted at both room temperature and liquid-nitrogen temperature to determine an experimental critical plane-strain stress-intensity factor ( $K_{Ie}$ ) for each type of flawed test specimen. The

average values of room-temperature  $K_{Ie}$  were used to determine the stress levels that were applied during the sustained-load stress-corrosion crack-growth tests as follows:

- (1) JPL specimens: nominal stress = 55%  $K_{Ie}$ .
- (2) AFSD specimens:
  - (a) Nominal stress = 60%  $K_{Ie}$ .
  - (b) Maximum stress = 70%  $K_{Ie}$ .
  - (c) Threshold stress = 80%  $K_{Ie}$ .

The sustained-load tests were preceded by two short-duration tensile-load tests with exposure to Freon PCA, which simulated the stress levels experienced by the propellant tanks during manufacturing leak tests and proof tests. These were followed by the sustained-load tests with exposure to Freon PCA for a duration of 1000 hours. After this, the Freon PCA was replaced in the test propellant system with NTO MON-1 and the sustained-load testing continued for another 1000 hours. In later tests, the exposure time for NTO MON-1 was extended to 2000 hours.

At the completion of the sustained-load tests, the flawed sections were marked and fractured for posttest analysis to determine the extent of crack propagation. A scanning electron microscope (SEM) was used to make photomicrographs of the specimen's fractured surface for morphological examination.

#### D. SCOPE OF PROGRAM

This program is based upon standard stress-corrosion crack-growth testing procedures. All tests and procedures involving solvent, propellant, and material combinations were comprehensive and included the following major categories:

- (1) Acquisition and inspection of test specimens.
- (2) Propellant assay.
- (3) Material properties certification.
- (4) Processing surface flaws and the precracking of specimens.
- (5) Pretest cleaning of specimens and propellant test systems.
- (6) Inert fracture tensile testing.
- (7) 1000- to 2000-hour-duration sustained load, solvent/propellant/material exposure tests.

- (8) Posttest analysis.
- (9) Conclusions and recommendations.

#### E. METHOD OF QUALIFICATION

The criteria and recommended practices in the design of metallic pressure vessels to minimize proof-test failures and prevent service-life failures (Refs. 3 and 4) provide a method to determine the subcritical flaw-growth data used to qualify the pressure vessels used in this program. Linear-elastic fracture mechanics provide the basic framework and engineering language for describing the fracture of materials under static, cyclic, and sustained-stress loading. The expressions used to calculate critical-flaw sizes for surface flaws in uniformly stressed thin-wall vessels are summarized in Appendix A. JPL has applied this method successfully to develop and qualify pressure vessels of Mariner-, Viking-, and Voyager-class spacecraft for unmanned exploration. Those previously developed analytical and experimental procedures, test equipment, and facilities were used without modifications in accomplishing the work for this AFSD program.

## SECTION II

### SOLVENT/PROPELLANT AND MATERIAL

#### A. SOLVENT/PROPELLANT PROCUREMENT

The Freon PCA solvent was supplied from existing stock on hand at JPL's Edwards Test Station (ETS). The propellant oxidizer NTO (or  $N_2O_4$ ) MON-1 was supplied by the Air Force Rocket Propulsion Laboratory (AFRPL) in JPL-prepared and -cleaned 1000-ml cylinders.

#### B. SOLVENT/PROPELLANT CHARACTERIZATION

Freon PCA is trichlorotrifluoroethane (1,1,2-trichloro-1,2,2 trifluoroethane), for which the applicable military specification is MIL-C-81302C, Type I - ultraclean, and the appropriate NASA specification is MSFC-SPEC-237A. The chemical formula is  $CCl_2F-CClF_2$ . It is described in Ref. 5 as a clear, colorless liquid, nonflammable, chemically and thermally stable, low in toxicity, and recoverable by distillation without decomposition. It has a boiling point of  $47.6^\circ C$  ( $117.6^\circ F$ ) and a freezing point of  $-35^\circ C$  ( $-31^\circ F$ ). At a temperature of  $25^\circ C$  ( $77^\circ F$ ), the density of the liquid is  $1.565 \text{ g/cm}^3$  ( $97.69 \text{ lb/ft}^3$ ) and the vapor pressure is 337 mm Hg (6.5 psia). The purity is 99.9% of weight with a residue of 1 ppm by weight (maximum); moisture content is 10 ppm by weight (maximum), chloride ion 0.1 ppm by weight (maximum), and an acid number of 0.003 mg KOH/g of sample (maximum). Freon PCA is used by Hughes Aircraft Company as both a cleaning solvent and a referee test fluid in the manufacture and qualification of NTO propellant tanks.

NTO is a highly regarded propellant oxidizer because it is very reactive chemically, thermally stable, and insensitive to mechanical shock and impact. Although nonflammable, it will react hypergolically with hydrazine and its derivative fuels. It is described in Ref. 6 as a volatile, heavy, reddish-brown liquid that boils at 294.35 K ( $70.1^\circ F$ ) and melts at 261.95 K ( $11.8^\circ F$ ). At a temperature of 298 K ( $77^\circ F$ ), the density of the liquid is  $1.433 \text{ g/cm}^3$  ( $34.364 \text{ lb/ft}^3$ ) and the vapor pressure is 898.57 mm Hg (17.38 psia).

NTO when mixed with nitric oxide (NO) forms MON-type oxidizers. MON-1 contains an addition of 0.6 to 1.0% NO to minimize stress-corrosion cracking of titanium-alloy propellant tanks. This low concentration of NO gives the mixture a green color. MON-1 has a slightly lower melting temperature of 260.3 K ( $8.9^\circ F$ ), a very slightly lower density, and a slightly higher vapor pressure than NTO. The NTO MON-1 used in these tests met the standard MIL-P-26539C Amendment 2, dated 6 April 1976. Pretest and posttest analyses are shown in Table 1.



Table 1. Nitrogen Tetroxide MON-1 Analyses

Constituent or Property	Specification (MIL-P-26539C, Amendment 2)	Pretest Results	Posttest Results
N <sub>2</sub> O <sub>4</sub> + NO assay % by weight	99.5 to 100.6	99.74	100.18
Nitric oxide, % by weight	0.8 ±0.2	1.20 <sup>a</sup>	1.19 <sup>a</sup>
Water, % by weight	0.17 max	0.04	0.0415
Chloride, % by weight	0.04 max	< 0.01	< 0.005
Particulate, mg/l	10	— <sup>b</sup>	< 10.8 <sup>c</sup>
Ash (NVR), % by weight	0.001	—	0.00075
Dissolved metals, ppm by weight			
Iron		—	0.18
Nickel		—	0.06
Chromium		—	0.06
Titanium		—	< 0.2 ND

<sup>a</sup>The nitric-oxide level was slightly higher than specifications; however, this was determined to be acceptable by AFSD.

<sup>b</sup>No data available.

<sup>c</sup>Calculated from nonvolatile residue (NVR).

### C. MATERIAL PROCUREMENT

The Ti-6Al-4V alloy test specimens supplied by JPL were fabricated at JPL from tank forgings purchased from Titanium Metals Corporation of America (TMCA) for the Mariner and Viking spacecraft. A total of nine specimens were provided. They consisted of three parent-metal, three center-of-weld, and three weld-heat-affected-zone samples finish machined per the JPL fracture mechanics test specification drawing given in Ref. 7.

The Ti-6Al-4V alloy test specimens supplied by AFSD were fabricated by Fansteel, Precision Sheet Metal, under subcontract from Hughes Aircraft Company. A total of 42 specimens were provided, all of which were tungsten-inert gas (TIG) weldments compatible with the JPL drawing of Ref. 7. The only exception was the central test section, which was finish machined on both sides to the actual tank-weld thickness of 0.114 cm (0.045 in.). A photograph of a typical test specimen is shown in Fig. 3.

### D. MATERIAL CHARACTERIZATION

#### 1. Chemical Composition

The Ti-6Al-4V alloy forgings from which the test specimens were fabricated were reported, by heat numbers, to have the following chemical compositions:

#### Chemical Analysis

Element <sup>a</sup>	Heat Number (Supplier)		
	G-804 (JPL)	K-2101 (JPL)	P-6539 (AFSD)
Al	6.2	6.4	6.1
V	4.1	4.3	4.4
C	0.023	0.022	0.024
Fe	0.14	0.17	0.18
O	0.14	0.13	0.14
N	0.011	0.010	0.012
H	0.007	0.009	0.012
Ti	Bal.	Bal.	Bal.

<sup>a</sup>Chemical composition by weight (% wt.)

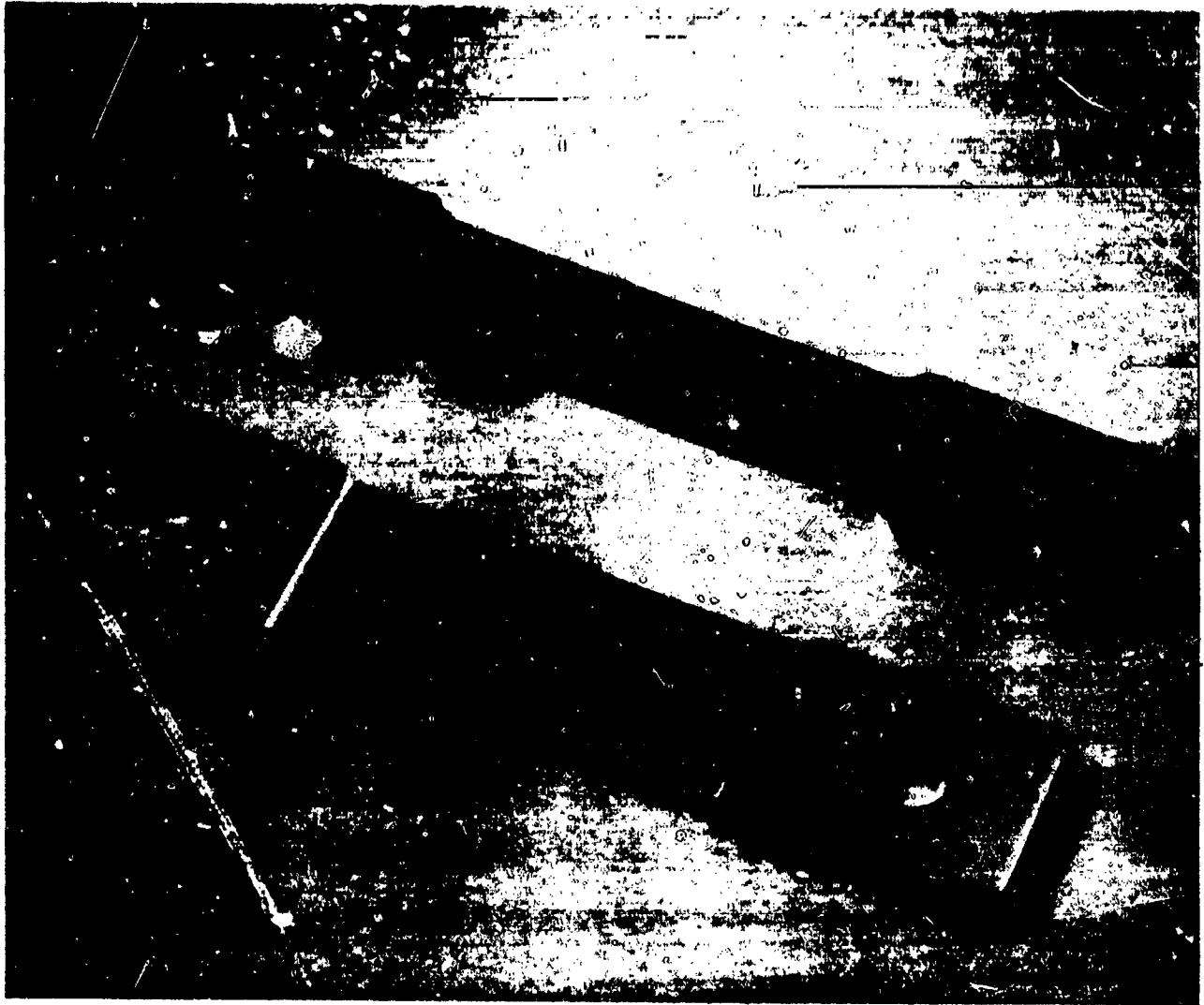


Figure 3. Typical AFSD Weldment Test Specimen

It is noted that the chemical composition of all three titanium-alloy heats are very comparable.

## 2. Mechanical Properties

The mechanical properties of the Ti-6Al-4V alloy specimens supplied by JPL in the solution heat-treated and aged (STA) condition were reported as follows:

Heat Number	YS, MPa (ksi)	UTS, MPa (ksi)	Elongation, %	Reduction of Area, %
G-804	1151 (167.0)	1256 (182.2)	12	44
K-2101	1134 (164.5)	1233 (178.8)	13	42

The mechanical properties of the Ti-6Al-4V alloy forging used by AFSD in the annealed condition were reported as follows:

Heat Number	YS, MPa (ksi)	UTS, MPa (ksi)	Elongation, %	Reduction of Area, %
P-6539	917 (133.0)	1000 (145.0)	20	48

The mechanical properties of the Ti-6Al-4V alloy test specimens supplied by AFSD in the STA condition were reported as follows:

Heat Number	YS <sup>a</sup> , MPa (ksi)	UTS, MPa (ksi)	Elongation, %	Reduction of Area, %
P-6539	1093 (158.5)	1147 (166.3)	14	47

<sup>a</sup>At room temperature of 21°C (70°F), the tensile yield strength ( $\sigma_{YS}$ ) values of 1103 MPa (160 ksi) for parent-metal and 965 MPa (140 ksi) for center-of-weld and weld-heat-affected-zone types of specimens in the STA conditions were used for calculations in this report.

### 3. Weldment Manufacturing Procedures

The sequence of manufacturing procedures used by Fansteel to fabricate weldment test specimens from forged girth-weld qualification rings follow:

- (1) Mults cut from bars of TMCA Ti-6Al-4V alloy.
- (2) Ring-roll forging of the mults into cylinders.
- (3) Annealing at 732.2°C (1350°F) in air for 2 hours and air cooling.
- (4) Rough machining to size.
- (5) Solution heat treatment at 954.4°C (1750°F) in air for 1-1/4 hours, water quenching within 6 seconds, partial aging at 537.8°C (1000°F) in air for 2 hours, and air cooling.
- (6) Finish machining to ring size.
- (7) Penetrant inspection using nonchlorinated solutions.
- (8) Preweld cleaning.
- (9) TIG welding of two rings together.
- (10) Visual, radiographic, penetrant, and dimensional inspection of weldments.
- (11) Weldment cleaning and final aging in vacuum at 621.1°C (1150°F) for 4 hours.
- (12) Weldments cut up, flattened, and finish machined to tensile test specimen size per the JPL drawing in Ref. 7.

### 4. Weldment Microstructure Examination

A photomicrograph of a typical TIG weldment section cut from a fabricated propellant tank made of Ti-6Al-4V alloy supplied by HAC is shown in Fig. 4. A photomicrograph of a finish-machined weldment section cut from a Ti-6Al-4V alloy test specimen is shown in Fig. 5. The microstructures of the weld nugget, heat-affected zone, and parent metal are typical for Ti-6Al-4V alloy TIG weldments. A favorable comparison can be made in the examinations of the actual tank weldment and the test specimen used in this program.

ORIGINAL PAGE IS  
OF POOR QUALITY

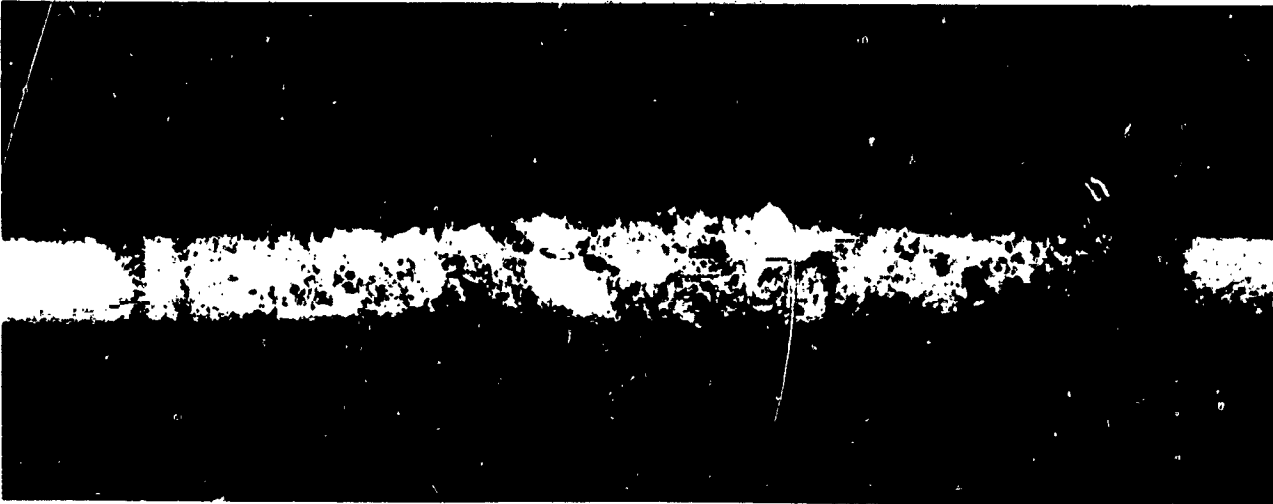


Figure 4. Typical HAC Propellant Tank Weldment Section  
(Courtesy of Hughes Aircraft Company)



Figure 5. Typical AFSD Test Specimen Weldment Section

## SECTION III

### TEST PROGRAM

#### A. TEST PROCEDURE

##### 1. Discussion

The test procedures used to determine stress-corrosion crack-growth sensitivity of Ti-6Al-4V alloy exposed to Freon FCA and NTO MON-1 are the same, with some minor modification, to those employed in previously completed fracture-mechanics programs sponsored by the Air Force Rocket Propulsion Laboratory (AFRPL), Refs. 8 and 9. The following detailed description is repeated here for the completeness of this report.

The weldment-type tensile-test specimens contained a part-through surface crack located either in the parent metal, center of weld, or weld-heat-affected zone. These flawed specimens were loaded in uniaxial tension to simulate the induced stresses resulting from pressure within a thin-wall propellant tank. Inert fracture tests with steadily increasing tensile loads at both room temperature and liquid-nitrogen temperature were used first to determine the experimental critical plane-strain, stress-intensity factor ( $K_{Ie}$ ) for each type of specimen containing one nominal flaw size. To evaluate stress-corrosion crack-growth sensitivity, the room-temperature values of  $K_{Ie}$  were then used to determine the sustained-load condition for the flawed specimens exposed sequentially to the active environments of Freon FCA and NTO MON-1. Three separate test series were performed; in these tests, the initial plane-strain stress intensity ( $K_{Ii}$ ) was increased in steps as follows:

Series Test No.	Specimen Source	Stress Intensity Level
1	JPL	Nominal, $K_{Ii} = 55\% K_{Ie}$
2	AFSD	Nominal, $K_{Ii} = 60\% K_{Ie}$
3	AFSD	Maximum, $K_{Ii} = 70\% K_{Ie}$
		Threshold, $K_{Ii} = 80\% K_{Ie}$

The choice of these conditions was based on test data reported in Ref. 10 where the threshold plane-strain stress-intensity factor ( $K_{TH}$ ) for continuous flaw growth in Ti-6Al-4V alloy in an inert room-temperature environment is 90% of the critical plain-strain stress-intensity factor ( $K_{Ic}$ ). In Ref. 11 the reported  $K_{TH}$  for parent-metal Ti-6Al-4V alloy exposed to NTO MON-1 was 83%  $K_{Ic}$ .

A SEM was used for both pretest and posttest analyses of the specimens' flawed surface. At high magnifications (1000X to 3000X) of SEM photomicrographs, it is possible to confirm the pretest presence of precracking at the bottom of the starter notch, but not the extent or depth of precracking. On the specimens' posttest fracture surface, it is possible to distinguish between the flaw growth caused by cyclic loading during pretest cracking and posttest cracking, and the flaw growth, if present, caused by stress-corrosion cracking resulting from exposure to an active environment. Sets of test specimens exposed to Freon PCA and then to gaseous nitrogen (GN<sub>2</sub>) in place of the NTO MON-1 or only to air during the sustained load testing were used as control samples for comparison in the SEM analyses.

## 2. Test Matrix

The test matrix covering the program implementation is shown in Table 2. A total of nine JPL test specimens were equally divided between three parent-metal, three center-of-weld, and three weld-heat-affected-zone types. A total of 42 AFSD test specimens were equally divided between 14 parent-metal, 14 center-of-weld, and 14 weld-heat-affected-zone types. Thirteen of each type were designated for testing, and one of each type remained as a spare for use where needed.

## B. TEST SPECIMEN PREPARATION

The JPL-supplied test specimens were obtained from existing stock on hand at JPL. They had already been prepared for testing with identification numbers, the test-section dimensions measured, starter notches, precracking, and by propellant cleaning. Table 3 summarizes the maximum- and minimum-applied cyclic stresses, the method of loading, and the number of cycles applied during the precracking process for these specimens. Precracking of each specimen was confirmed using SEM analysis; after precracking, the specimens were placed into the test program. The AFSD-supplied test specimens were hand delivered to JPL from HAC. Their preparation for test follows.

### 1. Pretest

All AFSD-supplied specimens were visually inspected and identified with part numbers engraved on both ends. Micrometer measurements were made of the test section thickness and width, and the cross-sectional area was calculated. Since all 42 specimens were identical, they were arbitrarily divided into three groups of 14 each and designated for surface-flaw locations as parent-metal, center-of-weld, or weld-heat-affected-zone position.



Table 2. Test Matrix

JPL Test Specimens						
Item No.	Test Type <sup>a</sup>	Environment <sup>b</sup>	Number and Type of Specimen			Stress Level
			Parent Metal	Center of Weld	Heat-Affected Zone	
1	IFA	Air	1	1	1	$K_{Ie}$
2	IFC	LN <sub>2</sub>	1	1	1	$K_{Ie}$
3	SCC	PCA/NTO	1	1	1	55% $K_{Ie}$
4	No. of Specimens		3	3	3	
5	Total No. of Specimens		9			
AFSD Test Specimens						
1	IFA	Air	3	3	3	$K_{Ie}$
2	IFC	LN <sub>2</sub>	3	3	3	$K_{Ie}$
3	SCC	PCA/NTO	2	2	2	60% $K_{Ie}$
4	SCC	PCA/GN <sub>2</sub>	1	1	1	60% $K_{Ie}$
5	SCC	PCA/NTO	2	2	2	70% $K_{Ie}$
6	SCC	Air	1	1	1	70% $K_{Ie}$
7	SCC	PCA/NTO	1	1	1	80% $K_{Ie}$
8	No. of Spares		1	1	1	
9	No. of Specimens		14	14	14	
10	Total No. of Specimens		42			

<sup>a</sup>IFA: inert fracture ambient, 21°C (70°F) increasing load.  
IFC: inert fracture cryogenic, -196°C (-320°F) increasing load.  
SCC: stress-corrosion cracking, 49°C (120°F) sustained load.

<sup>b</sup>Air: ambient, 21°C (70°F) or 49°C (120°F).  
LN<sub>2</sub>: liquid nitrogen, -196°C (-320°F).  
PCA/NTO: Freon PCA/NTO MON-1, 49°C (120°F), 206.8 N/cm<sup>2</sup> (300 psia).  
PCA/GN<sub>2</sub>: Freon PCA/gaseous nitrogen, 49°C (120°F), 206.8 N/cm<sup>2</sup> (300 psia).

Table 3. Pretest Cracking and Posttest Marking JPL Test Specimens<sup>a</sup>

Specimen Identification Type	Type of Test			Pretest Cracking			Posttest Marking		
	Inert Fracture	Sustained Load		Applied Stress Maximum/Minimum, MPa (ksi)	No. of Cycles		Applied Stress Maximum/Minimum, MPa (ksi)	No. of Cycles	
III-21-3-3-P	X			241/14 (35/2.1)	9,000				
III-21-5-3-P		X		241/14 (35/2.1)	9,000		310/19 (45/2.7)	9,000	
III-21-5-1-P	X			241/14 (35/2.1)	9,000				
244-C-1	X			241/14 (35/2.1)	9,000				
279-C-4		X		241/14 (35/2.1)	10,000				
257-C-6	X			241/14 (35/2.1)	9,000		310/19 (45/2.7)	20,000	
234-H-7	X			241/14 (35/2.1)	8,000				
257-H-9		X		241/14 (35/2.1)	12,000				
257-H-2	X			241/14 (35/2.1)	14,000		241/14 (35/2.1)	10,000	

<sup>a</sup>All specimens were tension loaded for both pretest cracking and posttest marking.

## 2. Starter Notches

A starter notch was made in each test specimen at the designated location using electric discharge machining (EDM). The starter notch was configured as a segment of a circle with a length approximately one-eighth the width and a depth approximately one-third the thickness of the specimen's test section. Location and size of the starter notch is shown schematically in Fig. 6. Several test specimens were chemically etched along the edge to confirm that the center of the TIG-weld nugget was nominally located in the center of the test section. Figure 5 is a photomicrograph of a typical TIG weldment. The weld nugget shown is approximately 0.64 cm (0.25 in.) wide, and the heat-affected zone extends about 0.70 cm (0.28 in.) on either side. The EDM starter notch for a heat-affected-zone specimen is located approximately 0.48 cm (0.19 in.) from the center of the weld nugget; for the parent-metal specimen, it is located 0.95 cm (0.38 in.) from the center of the weld nugget. Starter-notch locations on the three types of test specimens are shown in Fig. 7.

## 3. Precracking Flaw

The method of precracking used on these relatively thin test specimens was unidirectional flexural bending. In this method, the starter notch is placed on the outside of the unidirectional bend where maximum tensile stress occurs. The tensile stress is proportionately less at the bottom of the notch. At the center of the test specimen's cross section, the tensile stress is zero; it reverses to compression on the inside of the bend. This type of stress distribution produced a surface crack around the starter notch that in most cases was no deeper than one-half the test specimen's thickness. The Instron Model 1331 servo-hydraulic testing system used for precracking and the unidirectional beam-bending fixture with a test specimen installed are shown in Fig. 8.

Table 4 summarizes the maximum- and minimum-applied cyclic stresses, the method of loading, and number of cycles applied during the precracking process.

## 4. Extensometer Mounting Clips

Two small knife-edge-type metal clips were attached with epoxy cement to either side of the starter notch. These clips were used to mount the extensometer on those specimens used for inert fracture tests. They were attached also to specimens that had completed the sustained-load tests and the posttest marking; they were attached just prior to the final inert fracture tests. A crack-opening-displacement (COD) extensometer (MTS Corporation Model No. 632.02B-21), used to record induced strain within a range of 0.38 to 7.35 cm (0.15 to 3.0 in.), was placed between the clips. This COD gauge installed on a test specimen set up for an inert fracture test at liquid-nitrogen temperature is shown inside the environmental chamber in Fig. 9.

ORIGINAL PAGE 19  
OF POOR QUALITY

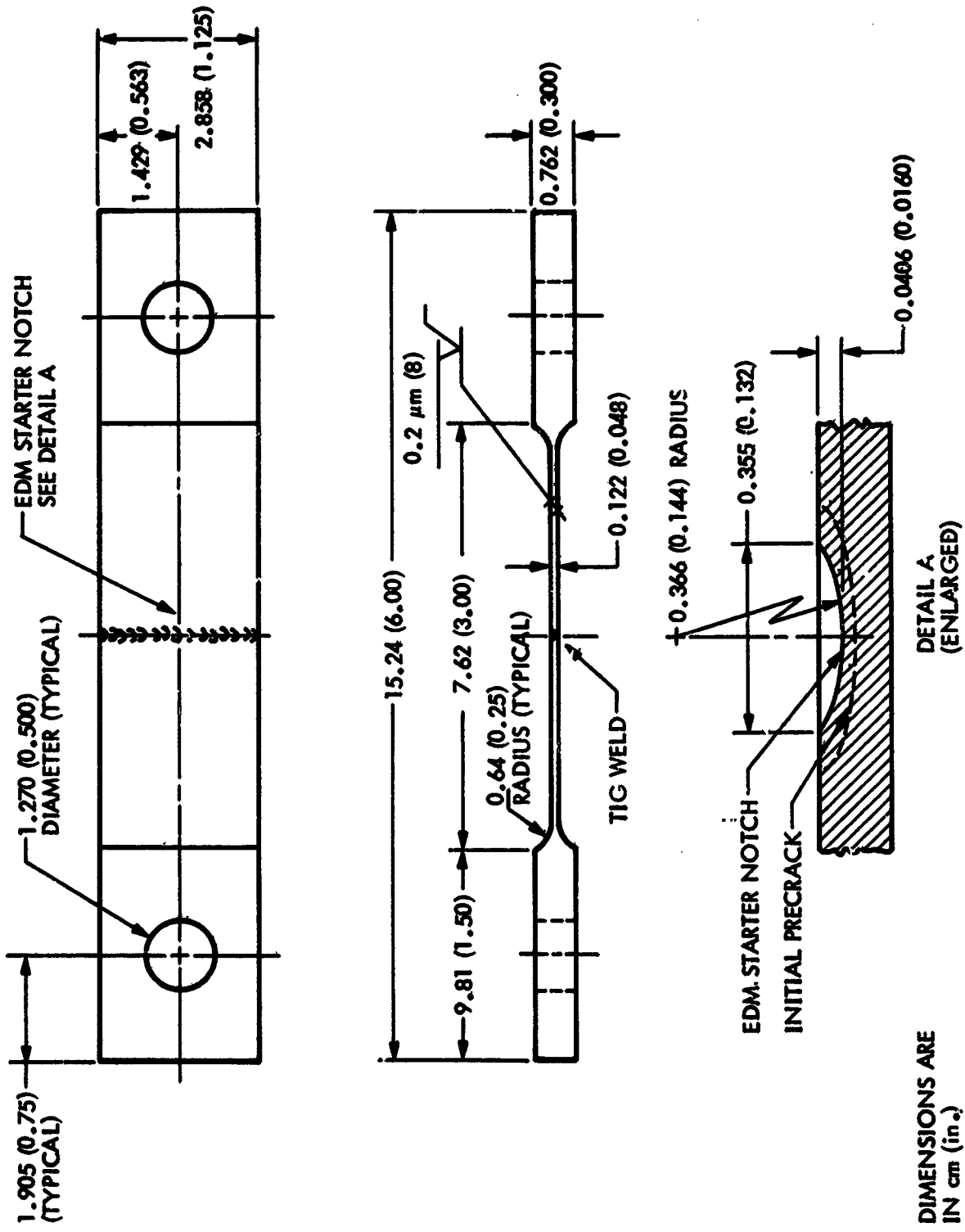


Figure 6. AFSD Test Specimen with EDM Starter Notch

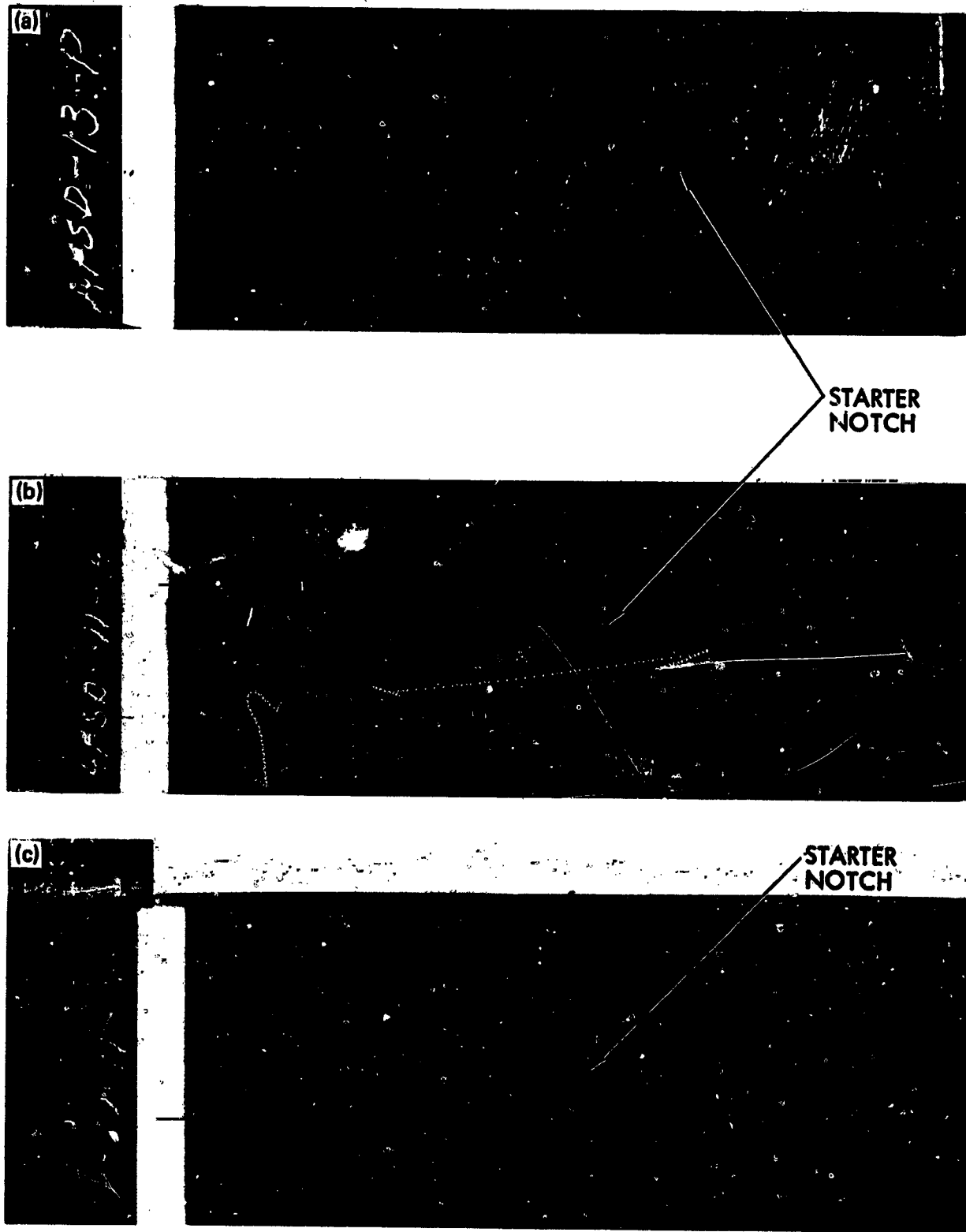


Figure 7. Typical Starter Notches in Three Types of AFSD Test Specimens: (a) Parent Metal; (b) Heat-Affected Zone; (c) Center Weld

ORIGINAL PAGE IS  
OF POOR QUALITY.



Figure 8. Instron Model 1331 Servo-Hydraulic Test System with Beam-Bending Fixture



Figure 9. MTS Systems Corporation Crack-Opening-Displacement-Type Extensometer Installed on Liquid-Nitrogen Inert Fracture Test Specimen

Table 4. Pretest Cracking and Posttest Marking AFSD Test Specimens<sup>a</sup>

Specimen Identification Type	Type of Test			Pretest Cracking			Posttest Marking		
	Inert Fracture	Sustained Load		Applied Stress Maximum/Minimum, MPa (ksi)	No. of Cycles		Applied Stress Maximum/Minimum, MPa (ksi)	No. of Cycles	
AFSD-01-P	X			172/52 (25/7.5)	12,000				
AFSD-02-P	X			517/117 (75/17)	30,000				
AFSD-03-P	X			517/117 (75/17)	50,000				
AFSD-04-P		X		517/117 (75/17)	30,000		172/10 (25/1.5)	1,000	
AFSD-05-P		X		517/117 (75/17)	30,000		345/21 (50/3.0)	500	
AFSD-06-P		X		517/117 (75/17)	30,000		517/31 (75/4.5)	1,000	
AFSD-08-P	X			517/117 (75/17)	30,000				
AFSD-09-P	X			345/103 (50/15)	90,000				
AFSD-10-P	X			345/103 (50/15)	60,000				
AFSD-11-P		X		345/103 (50/15)	50,000		103/6.2 (15/0.9)	1,000	
AFSD-12-P		X		345/103 (50/15)	50,000		172/10 (25/1.5)	1,000	
AFSD-13-P		X		345/103 (50/15)	50,000		103/6.2 (15/0.9)	500	
AFSD-14-P		X		345/103 (50/15)	50,000		103/6.2 (15/0.9)	500	
AFSD-01-C	X			345/103 (50/15)	20,000				
AFSD-02-C	X			517/117 (75/17)	30,000				
AFSD-03-C	X			517/117 (75/17)	50,000				
AFSD-04-C		X		517/117 (75/17)	30,000		172/10 (25/1.5)	500	
AFSD-05-C		X		517/117 (75/17)	30,000		345/21 (50/3.0)	500	
AFSD-06-C		X		517/117 (75/17)	30,000		345/21 (50/3.0)	500	
AFSD-08-C	X			517/117 (75/17)	30,000				
AFSD-09-C	X			345/103 (50/15)	90,000				
AFSD-10-C	X			345/103 (50/15)	60,000				
AFSD-11-C		X		345/103 (50/15)	50,000		103/6.2 (15/0.9)	500	
AFSD-12-C		X		345/103 (50/15)	50,000		172/10 (25/1.5)	1,000	
AFSD-13-C		X		345/103 (50/15)	50,000		103/6.2 (15/0.9)	500	
AFSD-14-C		X		345/103 (50/15)	50,000		103/6.2 (15/0.9)	1,000	

<sup>a</sup>All specimens were bending loaded for pretest cracking, and tension loaded for posttest marking.

Table 4. Pretest Cracking and Posttest Marking AFSD Test Specimens<sup>a</sup> (Continued)

Specimen Identification Type	Type of Test		Pretest Cracking		Posttest Marking	
	Luert Fracture	Sustained Load	Applied Stress Maximum/Minimum, MPa (ksi)	No. of Cycles	Applied Stress Maximum/Minimum, MPa (ksi)	No. of Cycles
AFSD-01-H	X		172/52 (25/7.5)	12,000		
AFSD-02-H	X		517/117 (75/17)	30,000		
AFSD-03-H	X		517/117 (75/17)	50,000		
AFSD-04-H		X	517/117 (75/17)	30,000	517/31 (75/4.5)	500
AFSD-05-H		X	517/117 (75/17)	30,000	345/21 (50/3.0)	500
AFSD-06-H		X	517/117 (75/17)	30,000	103/6.2 (15/0.9)	1,000
AFSD-08-H	X		517/117 (75/17)	30,000		
AFSD-09-H	X		345/103 (50/15)	90,000		
AFSD-10-H	X		345/103 (50/15)	60,000		
AFSD-11-H		X	345/103 (50/15)	50,000	103/6.2 (15/0.9)	500
AFSD-12-H		X	345/103 (50/15)	50,000	172/10 (25/1.5)	1,000
AFSD-13-H		X	345/103 (50/15)	50,000	103/6.2 (15/0.9)	500
AFSD-14-H		X	345/103 (50/15)	50,000	103/6.2 (15/0.9)	1,000

<sup>a</sup>All specimens were bending loaded for pretest cracking, and tension loaded for posttest marking.



## C. TESTING

### 1. Inert Fracture Tests

Inert fracture tests were conducted in the JPL Materials Laboratory using the MTS Systems Corporation Model 810 servo-hydraulic testing system. These tests were conducted at both room temperature (21°C (70°F)) and at liquid-nitrogen temperature (-196°C (-320°F)). The MTS system with the environmental chamber installed is shown in Fig. 10. A tensile load increasing steadily at a rate of 13.3 kN/min (3000 lb/min) was applied to each test specimen until failure occurred. The back surface of the flawed test section was visually monitored for evidence of localized plastic yielding (dimpling). Applied stress and induced strain (crack-opening displacement) were simultaneously recorded and graphed during these tests. Typical stress/strain (load-vs-displacement) curves for all three types of flawed specimens at both room temperature and liquid-nitrogen temperature are shown in Figs. 11, 12, and 13.

### 2. Stress-Corrosion Crack-Growth Tests

The sustained-load tests for determining the stress-corrosion crack-growth sensitivity of Ti-6Al-4V alloy exposed to Freon PCA and NTO MON-1 were conducted at JPL's Edwards Test Station (ETS). The six Satec Systems Incorporated Model C calibrated dead-load machines were used. Room temperatures were maintained at 49°C (120°F) throughout the test period.

Prior to installation into the machines, all test specimens were thoroughly propellant cleaned per JPL specification No. FS504574, Revision C. A propellant-cup test fixture, consisting of two propellant cups as shown in Fig. 14, was attached to each test specimen at the time of installation into the static testing machine. The two propellant cups, containing Teflon seal rings, were centered over the flawed section on each side of the test specimen and bolted together, as shown in Fig. 15. Belleville spring washers under the bolt heads maintained a constant sealing force. Leak tests using GN<sub>2</sub> were made to insure tightness of the test assemblies. The propellant exposure systems were completely vacuum purged and then charged with Freon PCA to 206.8 N/cm<sup>2</sup> (300 psia).

The sustained-load test series with exposure to Freon PCA began with two short-duration tests designed to simulate HAC's tank leak testing and proof testing. These were conducted according to the stress-level profiles shown sequentially in Fig. 16. A stress level of 172 MPa (25 ksi), which is equivalent to 690 kN/m<sup>2</sup> (100 psid) tank pressure, was applied in a single loading step and held for 40 hours. This load was then removed in a single step. After 8 hours, a steadily increasing load was applied over a 20-minute period up to a stress level of 690 MPa (100 ksi), which is equivalent to 2758 kN/m<sup>2</sup> (400 psid) tank pressure. This was held for only 5 minutes and then the load was steadily removed over a 10-minute period. Following these tests, the static loading on each machine was adjusted for the K<sub>I1</sub> levels calculated for the installed specimens according to the Table 2 Test Matrix. The sustained-stress testing with exposure to Freon PCA for 1000 hours was started with the direct application of this load.

ORIGINAL PAGE IS  
OF POOR QUALITY

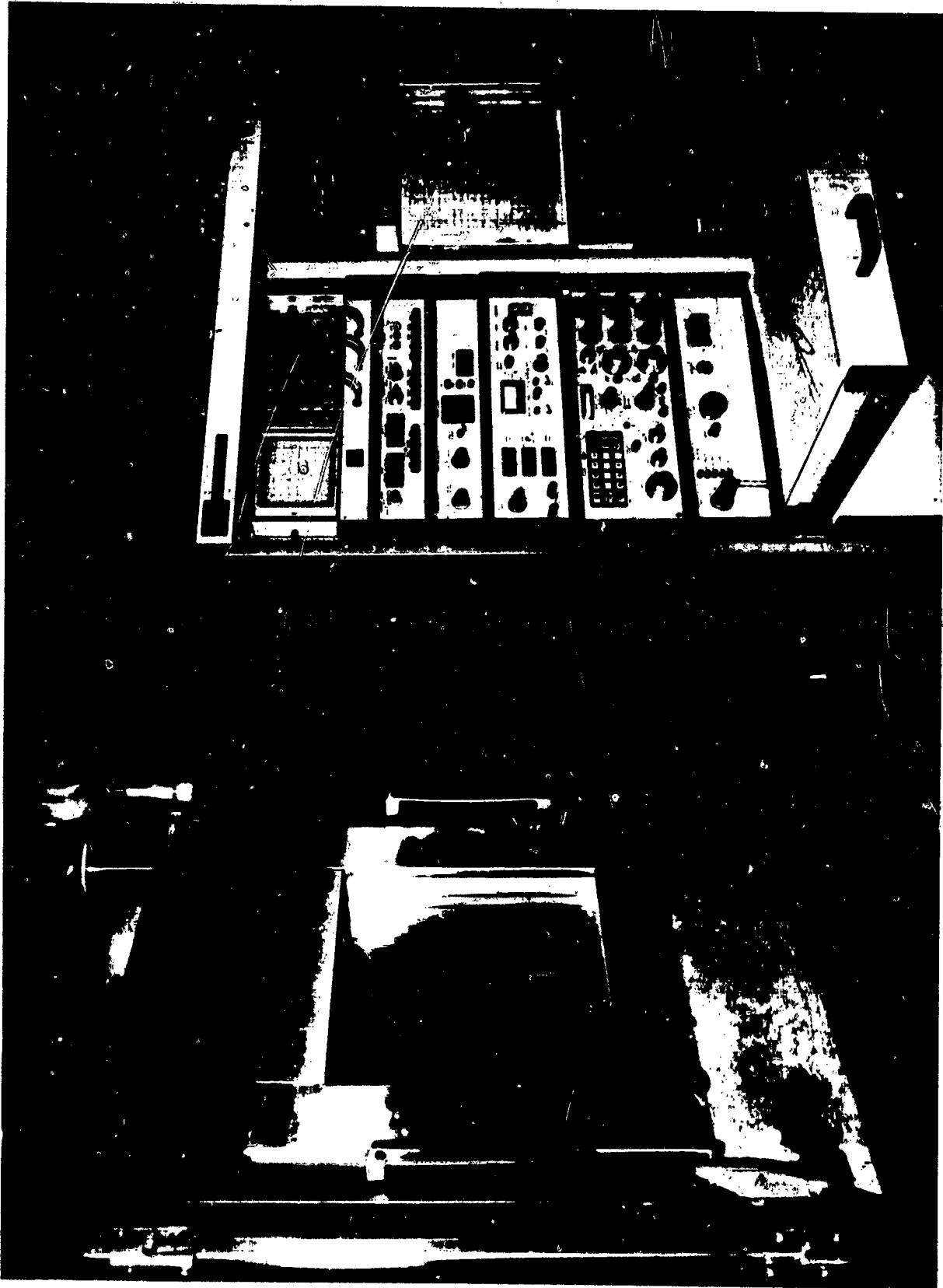


Figure 10. MTS Systems Corporation Model 810 Servo-Hydraulic Testing System with Environmental Chamber

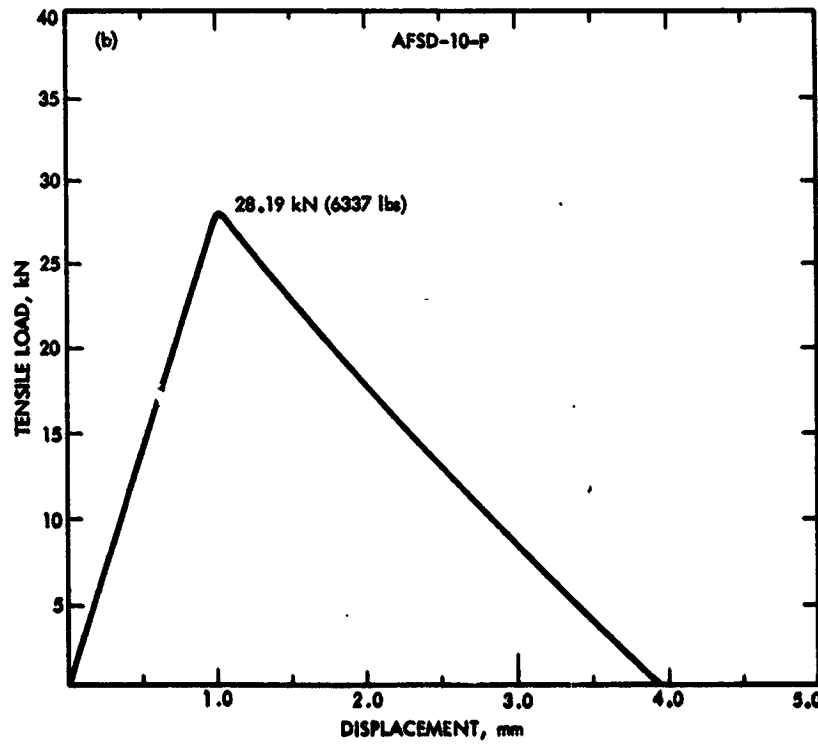
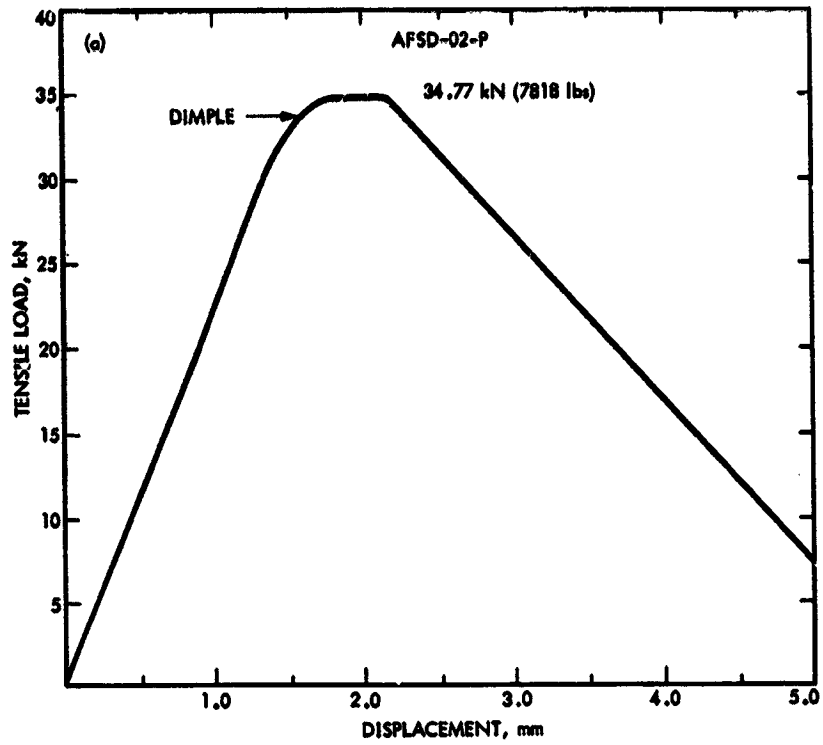


Figure 11. Typical Stress/Strain Curves for Parent-Metal-Specimen Inert Fracture Tests: (a) Room Temperature; (b) Liquid-Nitrogen Temperature

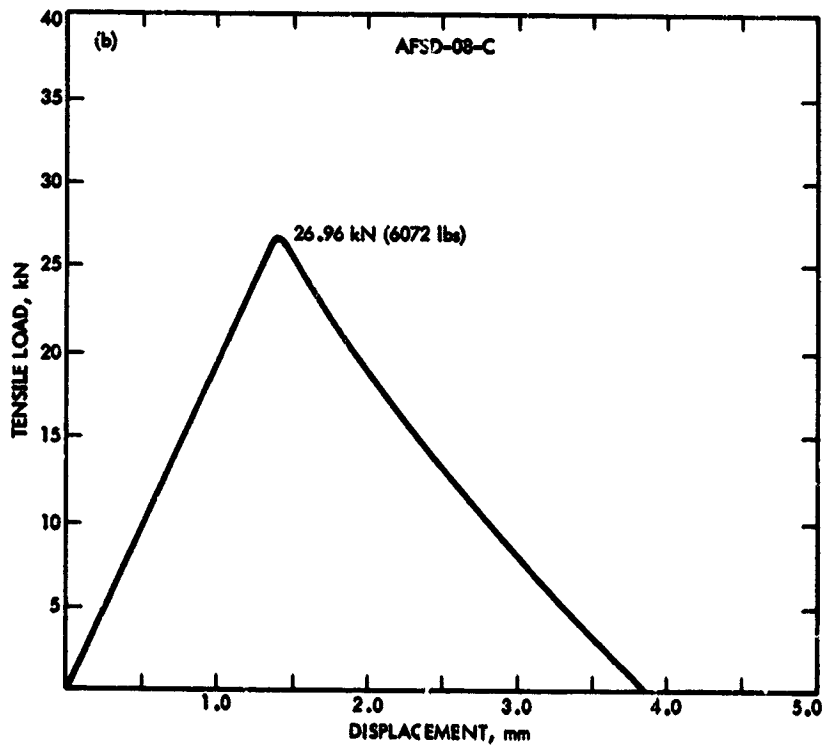
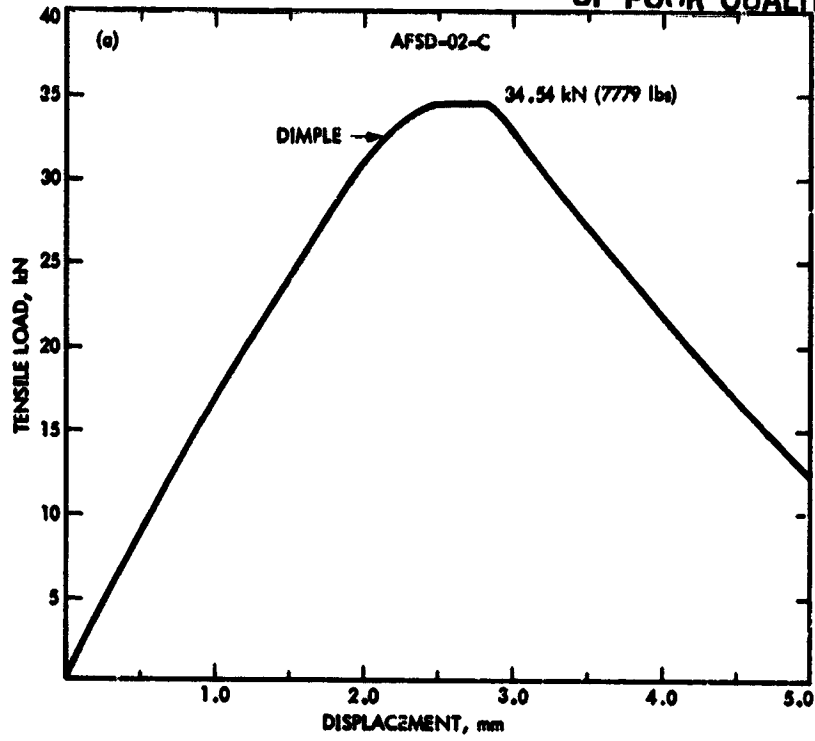


Figure 12. Typical Stress/Strain Curves for Center-Weld-Specimen Inert Fracture Tests: (a) Room Temperature; (b) Liquid-Nitrogen Temperature

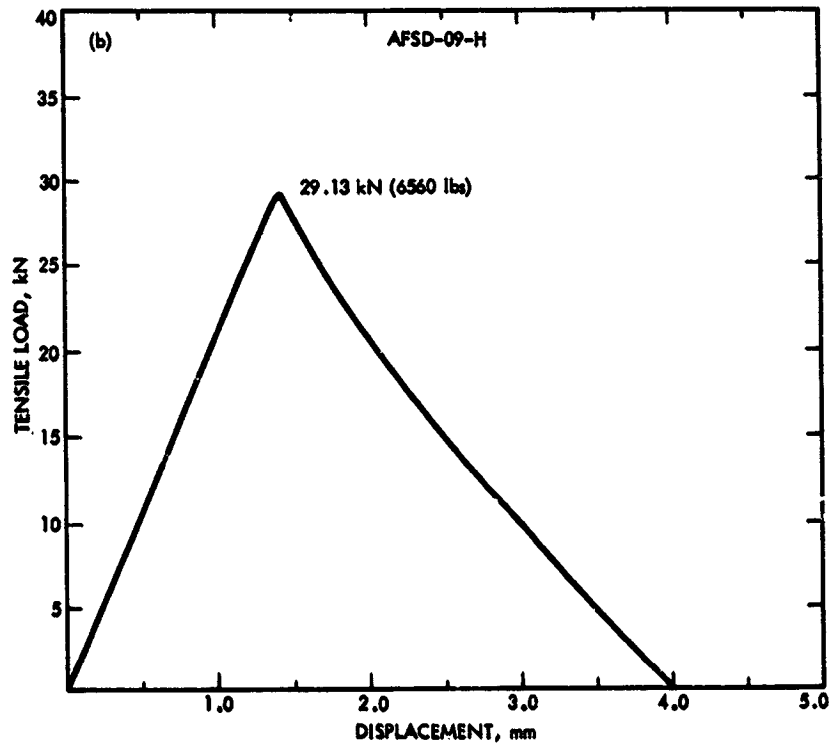
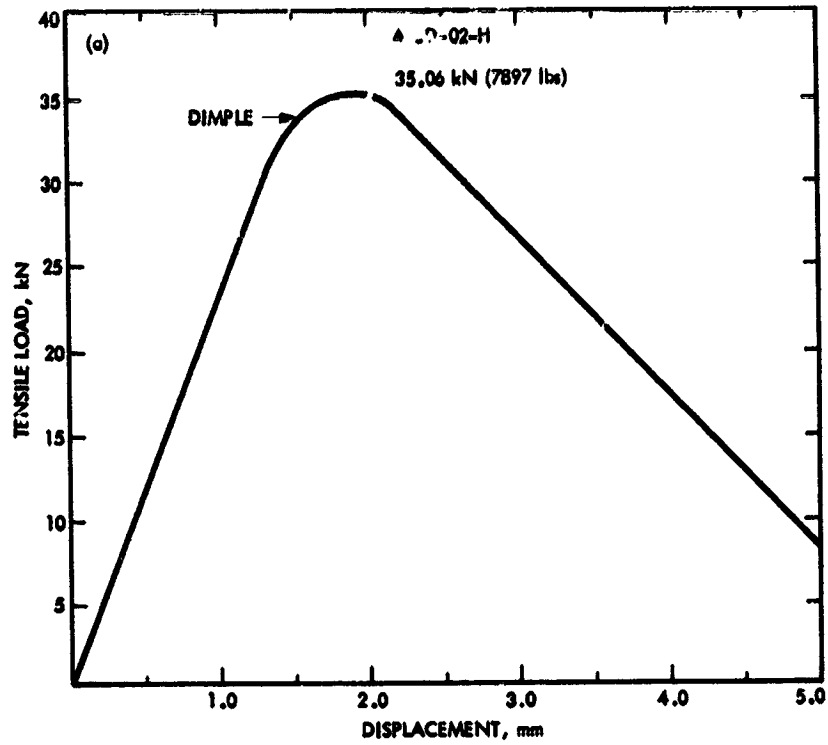


Figure 13. Typical Stress/Strain Curves for Heat-Affected-Zone-Specimen Inert Fracture Tests: (a) Room Temperature; (b) Liquid-Nitrogen Temperature

ORIGINAL PAGE IS  
OF POOR QUALITY

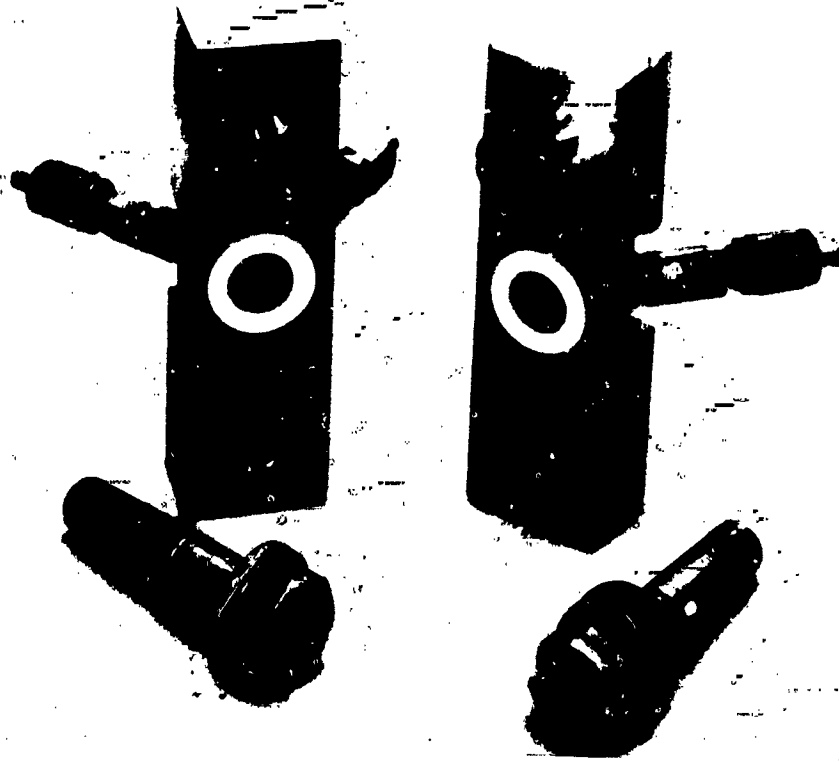


Figure 14. Propellant-Cup Test Fixture



Figure 15. Propellant-Cup Installed on Typical Test Specimen

ORIGINAL PAGE IS  
OF POOR QUALITY

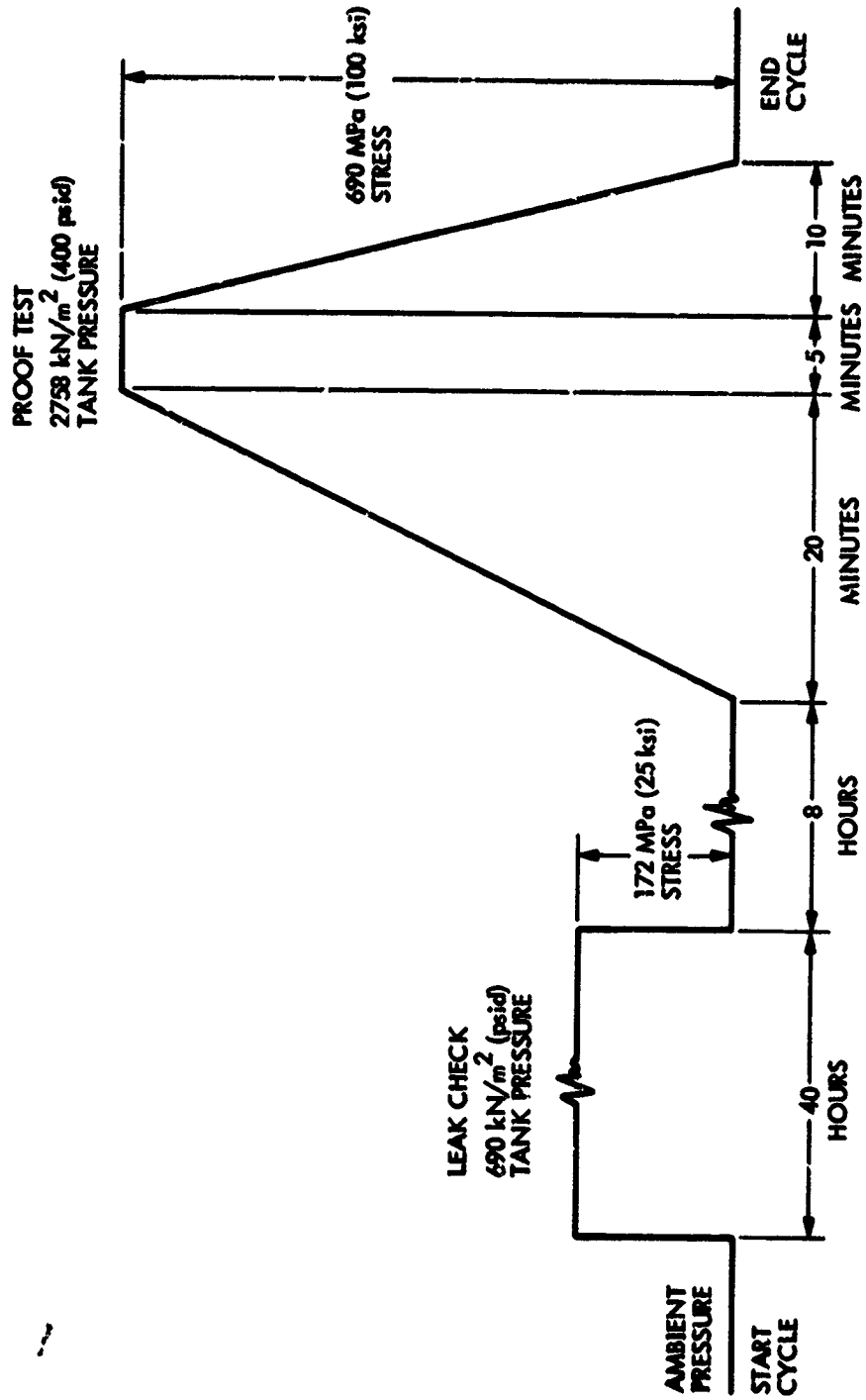


Figure 16. Stress-Level Profiles for Tank Leak Check and Proof Test

A photograph of the Satec Static-Load Test Machine Facility at ETS is shown in Fig. 17. Test assemblies consisting of mounting fixtures, two specimens installed in series, propellant cups and a propellant supply system are shown in Fig. 18. The make-up length between the two support pins on the mounting fixtures of each assembly was accurately measured before test loads were applied, after loading, and periodically during testing for evidence of specimen elongation resulting from crack growth or creep. Daily visual inspections were also made of all test assemblies.

After 1000 hours of exposure to Freon PCA, the static loads were temporarily removed. Freon PCA was purged from the propellant system using GN<sub>2</sub>. The Freon PCA supply cylinders were replaced with NTO MON-1 cylinders and the delivery system vacuum purged for 5 minutes. Designated test assemblies were filled with NTO MON-1 and pressurized to 206.8 N/cm<sup>2</sup> (300 psia). The control specimen test assemblies were pressurized to 206.8 N/cm<sup>2</sup> (300 psia) with GN<sub>2</sub>. Static loads were then reapplied to all test machines and the sustained-stress testing with exposure to NTO MON-1 continued for another 1000 hours.

After successfully completing the first test series using the JPL specimens, the second and third test series using AFSD specimens were extended to 2000 hours of sustained load with exposure to NTO MON-1. On the third test series, the three control specimens were exposed only to ambient air throughout the entire test period.

#### D. POSTTEST

##### 1. Test Termination

The sustained-load tests were terminated by first removing the applied loads. Propellant was drained from the test system and thoroughly purged with GN<sub>2</sub>. Specimens were removed from the test fixtures, visually inspected, and individually bagged to avoid contamination of the surface exposed to propellant. The bagged specimens were returned from ETS to the JPL Materials Laboratory for photographing as required and posttest marking.

##### 2. Posttest Marking

Posttest marking of the surface flaw was accomplished by applying additional cyclic loading to each specimen to produce a second distinctive fatigue crack that would identify the terminus of stress-corrosion crack-growth testing. Since unidirectional flexural bending was used for precracking, uniaxial tensile loading was used for posttest marking. This produced a different cyclic stress pattern that is readily distinguished from the pretest crack as viewed on the SEM photomicrographs. The applied loads and numbers of cycles were varied until the desired depth of posttest marking was achieved.

Table 4 summarizes the posttest marking procedures including the maximum and minimum stresses, the method used, and the number of cycles for AFSD test specimens.



ORIGINAL PAGE IS  
OF POOR QUALITY



Figure 17. Satec Systems Incorporated Model C Static-Load Testing Machine Facility

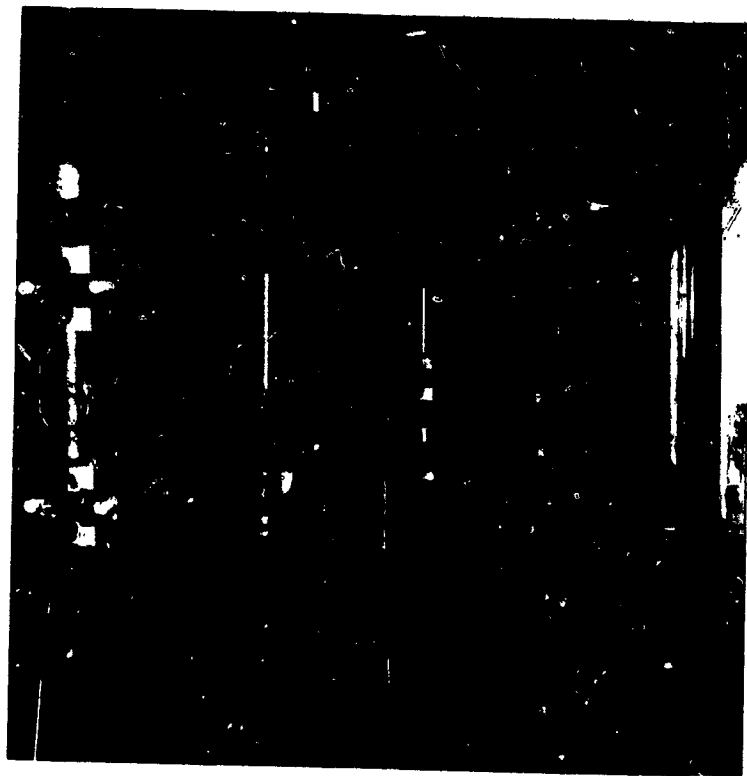


Figure 18. Typical Installation of Two Sustained-Load Test Specimens in Series

### 3. Posttest Fracture

The posttest-marked specimens from the sustained-load tests were prepared with mounting clips and extensometers in the same manner as those used for the inert fracture tests. Each specimen was then fractured at room temperature using a steadily increasing tensile load while recording the stress/strain data. A short length of the fractured section from one of the two halves of the test specimen was cut off, engraved with the specimen identification number, and used for SEM analysis for stress-corrosion crack growth.

## SECTION IV

### RESULTS

#### A. SUMMARY

It has been experimentally demonstrated that the propellant tank material Ti-6Al-4V alloy is insensitive to stress-corrosion crack growth when sequentially exposed to Freon PCA and NTO MON-1 at stress-intensity levels up to 80% of the experimental critical plane-strain stress-intensity factor ( $K_{Ie}$ ). None of the part-through surface-flawed type test specimens, including parent metal, center of weld, and weld heat affected zone, showed any crack growth resulting from sustained stress tests of 1000-hour duration while exposed to Freon PCA followed by 2000 hours while exposed to NTO MON-1.

#### B. INERT FRACTURE TESTS

The inert fracture test results for the nine JPL-supplied test specimens with surface flaws are presented in Table 5. These tests were made at both room temperature (21°C (70°F)) and at liquid-nitrogen temperature (-196°C (-320°F)). Size of the surface flaw and the experimental critical tensile stress at fracture were used to calculate  $K_{Ie}$  for each specimen according to the fracture-mechanics approach presented in Appendix A. The first specimen listed in each of the three groups, parent metal (P), center weld (C), and weld-heat-affected zone (H), is the one used for the room-temperature inert fracture test. The corresponding  $K_{Ie}$  was used to determine the initial stress intensity ( $K_{Ii}$ ) for the sustained-load test. The second specimen listed in each group is the one used for sustained-load testing, and the  $K_{Ie}$  was calculated from the posttest inert fracture. These values of  $K_{Ie}$  are valid because the posttest marking flaw depth did not exceed one-half the thickness of the test specimen ( $a/t < 0.50$ ). The last specimen in each group is the one used for the liquid-nitrogen-temperature inert fracture test. Fracture toughness at this cryogenic condition was lower for both the parent-metal and center-weld specimens, as expected. However, for the heat-affected-zone specimen, the value of  $K_{Ie}$  lies between the two room-temperature values; the reason is unclear.

Inert fracture test results for the eighteen AFSD-supplied test specimens with surface flaws are presented in Table 6. Three of each type specimen, P, C, and H, were fractured at room temperature and three each at liquid-nitrogen temperature. Size of the flaw and the critical tensile stress at fracture were again used to calculate  $K_{Ie}$  according to the method described in Appendix A. The average values of  $K_{Ie}$  are given in Table 7 for all three types of test specimens at both test temperatures. In making this average, only values of  $K_{Ie}$  were used where the flaw depth was less than 60% of the test-specimen thickness ( $a/t < 0.60$ ).

It should be acknowledged that these experimental values of  $K_{Ie}$  are for only one specimen thickness and one nominal flaw size. Many more similar tests with varying flaw sizes ( $a/Q$ ) are required to determine the generalized

Table 5. Inert Fracture Test Data for JPL Test Spec

Specimen Identification Type	Width w, cm (in.)	Thickness t, cm (in.)	Area A, cm <sup>2</sup> (in. <sup>2</sup> )	Load f <sub>e</sub> , kN (lbf)	Stress σ <sub>e</sub> , MPa (ksi)	Crack Depth a, cm (in.)	Crack Length 2c, cm (in.)	$\frac{a}{2c}$
III-21-3-3-P	2.5502 (1.0040)	0.2040 (0.0803)	0.5200 (0.0806)	60.49 (13,600)	1163.39 (168.73)	0.0442 (0.0174)	0.1676 (0.0660)	0.264
III-21-5-3-P	2.5512 (1.0044)	0.2037 (0.0802)	0.5194 (0.0805)	60.49 (13,600)	1164.84 (168.94)	0.0456 (0.0179)	0.2261 (0.0890)	0.201
III-21-5-1-P	2.5559 (1.0062)	0.2040 (0.0803)	0.5213 (0.0808)	71.61 (16,100)	1373.90 (199.26)	0.0264 (0.0104)	0.1720 (0.0677)	0.154
244-C-1	2.5558 (0.9028)	0.1537 (0.0605)	0.3529 (0.0547)	37.81 (8,500)	1071.41 (155.39)	0.0556 (0.0219)	0.2878 (0.1133)	0.193
279-C-4	2.2954 (0.9037)	0.1537 (0.0605)	0.3529 (0.0547)	34.65 (7,790)	981.92 (142.41)	0.0589 (0.0232)	0.3180 (0.1252)	0.185
257-C-6	2.2962 (0.9040)	0.1529 (0.0602)	0.3510 (0.0544)	29.36 (6,600)	836.50 (121.32)	0.0508 (0.0220)	0.2845 (0.1120)	0.196
234-H-7	2.2954 (0.9037)	0.1504 (0.0592)	0.3452 (0.0535)	36.74 (8,260)	1064.52 (154.39)	0.0711 (0.0286)	0.3048 (0.1200)	0.238
257-H-9	2.2901 (0.9016)	0.1504 (0.0592)	0.3445 (0.0534)	37.81 (8,500)	1097.55 (159.18)	0.0607 (0.0239)	0.3043 (0.1198)	0.199
257-H-2	2.2929 (0.9027)	0.1504 (0.0592)	0.3445 (0.0534)	48.93 (11,000)	1420.30 (205.99)	0.0472 (0.0186)	0.2939 (0.1157)	0.161

FOLDOUT FRAME

rt Fracture Test Data for JPL Test Specimens

Ess $\sigma_e$ , (ksi)	Crack Depth a, cm (in.)	Crack Length 2c, cm (in.)	$\frac{a}{2c}$	$\frac{\sigma_e}{\sigma_{YS}}$	$\frac{a}{t}$	Q	$\frac{a}{Q}$ , cm (in.)	$M_K$	$K_{Le}$ , MPa $\sqrt{m}$ (ksi $\sqrt{in.}$ )	Test Temperature, °C (°F)
3.39	0.0442	0.1676	0.264	1.054	0.127	1.28	0.0345	1.02	42.99	22
8.73)	(0.0174)	(0.0660)					(0.0136)		(39.12)	(72)
4.84	0.0456	0.2261	0.201	1.056	0.222	1.11	0.0409	1.02	46.87	22
8.94)	(0.0179)	(0.0890)					(0.0161)		(42.65)	(72)
3.90	0.0264	0.1720	0.154	0.830	0.130	1.33	0.0198	1.01	37.59	-196
9.26)	(0.0104)	(0.0677)					(0.0078)		(34.70)	(-320)
1.41	0.0556	0.2878	0.193	1.110	0.362	1.27	0.0437	1.05	45.92	22
5.39)	(0.0219)	(0.1133)					(0.0172)		(41.78)	(72)
1.92	0.0589	0.3180	0.185	1.017	0.383	1.31	0.0450	1.07	43.44	22
2.41)	(0.0232)	(0.1252)					(0.0177)		(39.53)	(72)
3.50	0.0508	0.2845	0.196	0.551	0.365	1.17	0.0478	1.07	38.14	-196
1.32)	(0.0220)	(0.1120)					(0.0188)		(34.70)	(-320)
4.52	0.0711	0.3048	0.238	1.103	0.483	1.21	0.0597	1.12	56.85	22
4.39)	(0.0286)	(0.1200)					(0.0235)		(51.73)	(72)
7.55	0.0607	0.3043	0.199	1.137	0.404	1.29	0.0470	1.08	50.15	22
3.18)	(0.0239)	(0.1198)					(0.0185)		(45.63)	(72)
0.30	0.0472	0.2939	0.161	0.936	0.314	1.37	0.0345	1.04	53.49	-196
3.99)	(0.0186)	(0.1157)					(0.0136)		(48.67)	(-320)

2 FOLDOUT FRAME

ORIGINAL PAGE IS  
OF POOR QUALITY

Table 6. Inert Fracture Test Data for AFSD Test Sp

Specimen Identification Type	Width w, cm (in.)	Thickness t, cm (in.)	Area A, cm <sup>2</sup> (in. <sup>2</sup> )	Load f <sub>e</sub> , kN (lbf)	Stress σ <sub>e</sub> , MPa (ksi)	Crack Depth a, cm (in.)	Crack Length 2c, cm (in.)	$\frac{a}{2c}$
AFSD-01-P	2.8555 (1.1242)	0.1217 (0.0479)	0.3471 (0.0538)	37.18 (8358)	1071.14 (155.35)	0.0452 (0.0178)	0.3396 (0.1337)	0.133
AFSD-02-P	2.8529 (1.1232)	0.1222 (0.0481)	0.3484 (0.0540)	34.77 (7818)	998.19 (144.77)	0.0521 (0.0205)	0.3622 (0.1426)	0.144
AFSD-03-P	2.8545 (1.1238)	0.1207 (0.0475)	0.3445 (0.0534)	27.13 (6100)	787.41 (114.23)	0.0925 (0.0364)	0.7071 (0.2784)	0.131
AFSD-08-P	2.8469 (1.1208)	0.1209 (0.0476)	0.3445 (0.0534)	21.47 (4827)	623.24 (90.3)	0.0742 (0.0292)	0.4867 (0.1916)	0.152
AFSD-09-P	2.8476 (1.1211)	0.1232 (0.0485)	0.3509 (0.0544)	37.36 (8400)	1064.66 (154.41)	0.0607 (0.0239)	0.3686 (0.1451)	0.165
AFSD-10-P	2.8486 (1.1215)	0.1199 (0.0472)	0.3413 (0.0529)	28.19 (6337)	825.95 (119.79)	0.0673 (0.0265)	0.4216 (0.1660)	0.165
AFSD-01-C	2.8479 (1.1212)	0.1201 (0.0473)	0.3419 (0.0530)	35.05 (7880)	1025.15 (148.68)	0.0404 (0.0159)	0.3239 (0.1275)	0.125
AFSD-02-C	2.8415 (1.1187)	0.1201 (0.0473)	0.3413 (0.0529)	34.60 (7779)	1008.19 (146.22)	0.1511 (0.0201)	0.3429 (0.1350)	0.149
AFSD-03-C	2.8514 (1.1226)	0.1204 (0.0474)	0.3432 (0.0532)	30.67 (6895)	893.66 (129.61)	0.0973 (0.0383)	0.4742 (.1867)	0.205
AFSD-08-C	2.8471 (1.1209)	0.1229 (0.0484)	0.3503 (0.0543)	27.01 (6072)	771.00 (111.82)	0.0749 (0.0295)	0.3861 (0.1520)	0.194
AFSD-09-C	2.8525 (1.1230)	0.1201 (0.0473)	0.3426 (0.0531)	26.19 (5889)	764.66 (110.90)	0.0602 (0.0237)	0.3838 (0.1511)	0.157
AFSD-10-C	2.8479 (1.1212)	0.1196 (0.0471)	0.3407 (0.0528)	27.99 (6292)	821.68 (119.17)	0.0579 (0.0228)	0.3828 (0.1507)	0.151
AFSD-01-H	2.8593 (1.1257)	0.1219 (0.0480)	0.3484 (0.0540)	36.65 (8240)	1052.11 (152.59)	0.0416 (0.0164)	0.3388 (0.1334)	0.123
AFSD-02-H	2.8504 (1.1222)	0.1232 (0.0485)	0.3510 (0.0544)	35.13 (7897)	1000.88 (145.16)	0.0508 (0.0200)	0.3284 (0.1293)	0.155
AFSD-03-H	2.8568 (1.1247)	0.1224 (0.0482)	0.3497 (0.0542)	0.3497 (6978)	31.04 (128.74)	0.0747 (0.0294)	0.4997 (0.1967)	0.150
AFSD-08-H	2.8558 (1.1243)	0.1219 (0.0480)	0.3484 (0.0540)	0.3484 (5190)	23.09 (96.11)	0.0719 (0.0283)	0.5037 (0.1983)	0.143
AFSD-09-H	2.8547 (1.1239)	0.1232 (0.0485)	0.3516 (0.0545)	0.3516 (6560)	29.18 (120.36)	0.0549 (0.0216)	0.3988 (0.1570)	0.138
AFSD-10-H	2.8540 (1.1236)	0.1189 (0.0468)	0.3394 (0.0526)	0.3394 (6429)	28.60 (122.22)	0.0518 (0.0204)	0.3701 (0.1457)	0.140

FOLDOUT FRAME

ORIGINAL PAGE IS  
OF POOR QUALITY

Fracture Test Data for AFSD Test Specimens

$\sigma_e$ , ksi	Crack Depth a, cm (in.)	Crack Length 2c, cm (in.)	$\frac{a}{2c}$	$\frac{\sigma_e}{\sigma_{YS}}$	$\frac{a}{t}$	Q	$\frac{a}{Q}$ , cm (in.)	$M_K$	$K_{Ie}$ , MPa $\sqrt{m}$ (ksi $\sqrt{in.}$ )	Test Temperature, °C (°F)
.14	0.0452	0.3396	0.133	0.971	0.372	0.97	0.0467	1.08	48.70	22
.35)	(0.0178)	(0.1337)					(0.0184)		(44.31)	(72)
.19	0.0521	0.3622	0.144	0.905	0.437	1.03	0.0505	1.13	49.24	22
.77)	(0.0205)	(0.1426)					(0.0199)		(44.80)	(72)
.41	0.0925	0.7071	0.131	0.714	0.766	1.05	0.0876	1.46	66.36	22
.23)	(0.0364)	(0.2784)					(0.0345)		(60.38)	(72)
.24	0.0742	0.4867	0.152	0.377	0.613	1.18	0.0627	1.28	55.32	-196
39)	(0.0292)	(0.1916)					(0.0247)		(50.34)	(-320)
.66	0.0607	0.3686	0.165	0.643	0.493	1.14	0.0531	1.16	39.00	-196
.41)	(0.0239)	(0.1451)					(0.0209)		(35.49)	(-320)
.95	0.0673	0.4216	0.165	0.499	0.568	1.18	0.0566	1.21	46.81	-196
.79)	(0.0265)	(0.1660)					(0.0227)		(42.59)	(-320)
.15	0.0404	0.3239	0.125	1.064	0.338	0.93	0.0437	1.07	44.52	22
.68)	(0.0159)	(0.1275)					(0.0172)		(40.51)	(72)
.19	0.1511	0.3429	0.149	1.044	0.425	0.99	0.0513	1.11	49.42	22
.22)	(0.0201)	(0.1350)					(0.0202)		(44.97)	(72)
.66	0.0973	0.4742	0.205	0.926	0.808	1.15	0.0846	1.41	71.46	22
.61)	(0.0383)	(.1867)					(0.0333)		(65.02)	(72)
.00	0.0749	0.3861	0.194	0.508	0.610	1.26	0.0594	1.23	45.08	-196
.82)	(0.0295)	(0.1520)					(0.0234)		(41.02)	(-320)
.66	0.0602	0.3838	0.157	0.504	0.501	1.16	0.0518	1.16	39.40	-196
.90)	(0.0237)	(0.1511)					(0.0204)		(35.85)	(-320)
.68	0.0579	0.3828	0.151	0.542	0.484	1.16	0.0500	1.15	41.18	-196
.17)	(0.0228)	(0.1507)					(0.0197)		(37.47)	(-320)
.11	0.0416	0.3388	0.123	1.090	0.342	0.93	0.0447	1.06	46.03	22
.59)	(0.0164)	(0.1334)					(0.0176)		(41.88)	(72)
.88	0.0508	0.3284	0.155	1.037	0.412	1.06	0.0480	1.10	47.00	22
.16)	(0.0200)	(0.1293)					(0.0189)		(42.77)	(72)
.04	0.0747	0.4997	0.150	0.920	0.602	1.08	0.0724	1.26	58.71	22
.74)	(0.0294)	(0.1967)					(0.0285)		(53.42)	(72)
.09	0.0719	0.5037	0.143	0.437	0.590	1.18	0.0610	1.25	39.86	-196
.11)	(0.0283)	(0.1983)					(0.0240)		(36.27)	(-320)
.18	0.0549	0.3988	0.138	0.547	0.445	1.12	0.0490	1.13	40.49	-196
.36)	(0.0216)	(0.1570)					(0.0193)		(36.84)	(-320)
.60	0.0518	0.3701	0.140	0.556	0.436	1.12	0.0462	1.13	39.93	-196
.2.22)	(0.0204)	(0.1457)					(0.0182)		(36.33)	(-320)

2 FOLDOUT FRAME

Table 7. Average Values of  $K_{Ie}$  for AFSD Test Specimens

Type of Specimen	Test Temperature, °C (°F)	$K_{Ie}$ , MPa $\sqrt{m}$ (ksi $\sqrt{in.}$ )
Parent Metal	21 (70)	49.25 (44.81)
Center Weld	21 (70)	47.02 (42.78)
Heat-Affected Zone	21 (70)	46.55 (42.36)
Parent Metal	-196 (-320)	42.90 (39.04)
Center Weld	-196 (-320)	40.29 (36.66)
Heat-Affected Zone	-196 (-320)	40.09 (36.48)

material toughness property identified as the critical plane-strain stress-intensity factor ( $K_{Ic}$ ) for this specimen thickness.

### C. STRESS-CORROSION CRACK-GROWTH TESTS

The nominal sustained-load test results to determine stress-corrosion crack-growth sensitivity for three JPL-supplied specimens are presented in Table 8. One of each type of surface-flawed specimen was exposed to Freon PCA for the leak-test and proof-test cycles and a sustained load for 1000 hours. This was followed by 1000 hours of sustained load with exposure to NTO MON-1. All tests were performed at a constant temperature of 49°C (120°F). None of the three specimens showed any evidence of crack growth at stress-intensity ratios ( $K_{I1}/K_{Ie}$ ) ranging from 0.545 to 0.660.

The nominal sustained-load test results for nine AFSD-supplied specimens are presented in Table 9. Two each of the three types of surface-flawed specimens were exposed to Freon PCA for the leak-test and proof-test cycles and a sustained load for 1000 hours. This was followed by 2000 hours of sustained load with exposure to NTO MON-1. The remaining three surface-flawed specimens, one of each type, were tested in the same manner except that NTO MON-1 was replaced by GN<sub>2</sub> for the final 2000 hours of testing to provide control samples. Stress-intensity ratios for these tests range from 0.593 to 0.677. None of the nine specimens showed any evidence of stress-corrosion crack growth.

The maximum sustained-load test results for the remaining twelve AFSD-supplied test specimens are presented in Table 10. All twelve surface-flawed specimens were exposed only to air during the leak-test and proof-test cycles so that the applied load that caused backface dimpling could be visually observed and recorded. After this was completed, the sustained-load testing with exposure to Freon PCA and NTO MON-1 proceeded as in previous tests. Nine specimens, three of each type, were exposed to Freon PCA for 1000 hours and then to NTO MON-1 for 2000 hours. The last three specimens, one of each type for use as control samples, were exposed only to air throughout the entire



ORIGINAL PAGE IS  
OF POOR QUALITY

Table 8. Nom

Specimen Identification Type	Width w, cm (in.)	Thickness t, cm (in.)	Area A, cm <sup>2</sup> (in. <sup>2</sup> )	Sustained Load f <sub>1</sub> , kN (lbf)	Sustained Stress σ <sub>1</sub> , MPa (ksi)	Initial Crack Depth a <sub>1</sub> , cm (in.)	Initial Length cm (in.)
III-21-5-3-P	2.5512 (1.0044)	0.2037 (0.0802)	0.5194 (0.0805)	38.12 (8570)	734.04 (106.46)	0.0356 (0.0140)	0.2 (0.0)
297-C-4	2.2954 (0.9037)	0.1537 (0.0605)	0.3529 (0.0547)	24.33 (5470)	689.50 (100.00)	0.0518 (0.0204)	0.3 (0.1)
257-H-9	2.2901 (0.9016)	0.1504 (0.0592)	0.3445 (0.0534)	23.75 (5340)	689.50 (100.00)	0.0490 (0.0193)	0.3 (0.1)

<sup>a</sup>Value of K<sub>Ie</sub> obtained from Table 5.

Table 9. Nom

Specimen Identification Type	Width w, cm (in.)	Thickness t, cm (in.)	Area A, cm <sup>2</sup> (in. <sup>2</sup> )	Sustained Load f <sub>1</sub> , kN (lbf)	Sustained Stress σ <sub>1</sub> , MPa (ksi)	Initial Crack Depth a <sub>1</sub> , cm (in.)	Initial Length cm (in.)
AFSD-04-P	2.8545 (1.1238)	0.1222 (0.0481)	0.3490 (0.0541)	19.75 (4400)	560.77 (81.33)	0.0630 (0.0248)	
AFSD-05-P	2.8486 (1.1215)	0.1237 (0.0487)	0.3523 (0.0546)	19.75 (4400)	555.67 (80.59)	0.0673 (0.0265)	
AFSD-06-P	2.8497 (1.1219)	0.1212 (0.0477)	0.3452 (0.0535)	19.35 (4350)	560.63 (81.31)	0.0721 (0.0284)	
AFSD-04-C	2.8550 (1.1240)	0.1277 (0.0483)	0.3503 (0.0543)	18.77 (4220)	592.78 (77.27)	0.0610 (0.0240)	
AFSD-05-C	2.8575 (1.1250)	0.1237 (0.0487)	0.3536 (0.0548)	18.77 (4220)	530.98 (77.01)	0.0724 (0.0285)	
AFSD-06-C	2.8466 (1.1207)	0.1217 (0.0479)	0.3536 (0.0537)	18.37 (4130)	530.29 (76.91)	0.0709 (0.0279)	
AFSD-04-H	2.8527 (1.1231)	0.1224 (0.0482)	0.3490 (0.0541)	18.28 (4110)	522.85 (75.83)	0.0749 (0.0295)	
AFSD-05-H	2.8469 (1.1208)	0.1227 (0.0483)	0.3490 (0.0541)	18.28 (4110)	523.81 (75.97)	0.0737 (0.0290)	
AFSD-06-H	2.8494 (1.1218)	0.1227 (0.0483)	0.3497 (0.0542)	18.28 (4110)	522.85 (75.83)	0.0671 (0.0264)	

<sup>a</sup>Value of K<sub>Ie</sub> obtained from Table 7.

FOLDOUT FRAME

Table 8. Nominal Sustained-Load Flaw-Growth Test Data for JPL Specimens

Initial Crack Depth $a_i$ , cm (in.)	Initial Crack Length $2c_i$ , cm (in.)	Final Crack Depth $a_f$ , cm (in.)	Final Crack Length $2c_f$ , cm (in.)	Flaw Growth $a_f - a_i$ , cm (in.)	$\frac{a_i}{2c_i}$	$\frac{\sigma_1}{\sigma_{YS}}$	$\frac{a_i}{t}$	$Q_1$	$\frac{a_i}{Q_1}$ cm (in.)
0.0356 (0.0140)	0.2240 (0.0882)	0.0356 (0.0140)	0.2240 (0.0882)	0	0.159	0.666	0.175	1.14	0.031 (0.012)
0.0518 (0.0204)	0.3089 (0.1216)	0.0518 (0.0204)	0.3089 (0.1216)	0	0.168	0.714	0.337	1.28	0.040 (0.015)
0.0490 (0.0193)	0.3035 (0.1195)	0.0490 (0.0193)	0.3035 (0.1195)	0	0.162	0.714	0.326	1.28	0.038 (0.015)

Table 9. Nominal Sustained-Load Flaw-Growth Test Data for AFSD Specimens

Initial Crack Depth $a_i$ , cm (in.)	Initial Crack Length $2c_i$ , cm (in.)	Final Crack Depth $a_f$ , cm (in.)	Final Crack Length $2c_f$ , cm (in.)	Flaw Growth $a_f - a_i$ , cm (in.)	$\frac{a_i}{2c_i}$	$\frac{\sigma_1}{\sigma_{YS}}$	$\frac{a_i}{t}$	$Q_1$	gm	
77 (0.0248)	0.0630 (0.0248)	0.3800 (0.1496)	0.0630 (0.0248)	0.3800 (0.1496)	0	0.166	0.508	0.516	1.16	0.
67 (0.0265)	0.0673 (0.0265)	0.3538 (0.1393)	0.0673 (0.0265)	0.3528 (0.1393)	0	0.190	0.504	0.544	1.24	0.
63 (0.0284)	0.0721 (0.0284)	0.4143 (0.1631)	0.0721 (0.0284)	0.4143 (0.1631)	0	0.174	0.508	0.595	1.20	0.
78 (0.0240)	0.0610 (0.0240)	0.3909 (0.1539)	0.0610 (0.0240)	0.3909 (0.1539)	0	0.156	0.555	0.497	1.16	0.
98 (0.0285)	0.0724 (0.0285)	0.4476 (0.1762)	0.0724 (0.0285)	0.4476 (0.1762)	0	0.162	0.550	0.585	1.16	0.
29 (0.0279)	0.0709 (0.0279)	0.3945 (0.1553)	0.0709 (0.0279)	0.3945 (0.1553)	0	0.180	0.549	0.583	1.20	0.
85 (0.0295)	0.0749 (0.0295)	0.4422 (0.1741)	0.0749 (0.0295)	0.4422 (0.1741)	0	0.169	0.542	0.611	1.18	0.
81 (0.0290)	0.0737 (0.0290)	0.4041 (0.1591)	0.0737 (0.0290)	0.4041 (0.1591)	0	0.182	0.543	0.600	1.21	0.
85 (0.0264)	0.0671 (0.0264)	0.4318 (0.1700)	0.0671 (0.0264)	0.4318 (0.1700)	0	0.155	0.542	0.547	1.15	0.

2 FOLDOUT FRAME

ORIGINAL PAGE IS  
OF POOR QUALITY

specimens

$\frac{a_1}{2c_1}$	$\frac{\sigma_1}{\sigma_{YS}}$	$\frac{a_1}{t}$	$Q_1$	$\frac{a_1}{Q_1}$ , cm (in.)	$M_{K1}$	$K_{I1}$ , MPa $\sqrt{m}$ (ksi $\sqrt{in.}$ )	$\frac{K_{I1}}{K_{Ie}}$	Duration of Test, h	Exposure Environment
.159	0.666	0.175	1.14	0.0312 (0.0123)	1.01	25.54 (23.24)	0.545	1002 1032	Freon PCA NTO MON-1
.168	0.714	0.337	1.28	0.0404 (0.0159)	1.06	28.67 (26.09)	0.660	1002 1032	Freon PCA NTO MON-1
.162	0.714	0.326	1.28	0.0384 (0.0151)	1.06	27.88 (25.37)	0.556	1002 1031	Freon PCA NTO MON-1

specimens

$\frac{a_1}{2c_1}$	$\frac{\sigma_1}{\sigma_{YS}}$	$\frac{a_1}{t}$	$Q_1$	$\frac{a_1}{Q_1}$ , gm (in.)	$M_{K1}$	$K_{I1}$ , MPa $\sqrt{m}$ (ksi $\sqrt{in.}$ )	$\frac{K_{I1}}{K_{Ie}}$	Duration of Test, H	Exposure Environment
0.166	0.508	0.516	1.16	0.0546 (0.0215)	1.16	29.52 (26.86)	0.599	1005 2012	Freon PCA NTO MON-1
0.190	0.504	0.544	1.24	0.0544 (0.0214)	1.18	29.71 (27.03)	0.603	1005 2012	Freon PCA NTO MON-1
0.174	0.508	0.595	1.20	0.0602 (0.0237)	1.23	32.92 (29.95)	0.668	1005 2012	Freon PCA GN <sub>2</sub>
0.156	0.555	0.497	1.16	0.0528 (0.0208)	1.16	27.85 (25.34)	0.593	1005 2012	Freon PCA NTO MON-1
0.162	0.550	0.585	1.16	0.0625 (0.0246)	1.23	31.82 (28.95)	0.677	1005 2012	Freon PCA NTO MON-1
0.180	0.549	0.583	1.20	0.0592 (0.0233)	1.22	30.59 (27.83)	0.651	1005 2012	Freon PCA GN <sub>2</sub>
0.169	0.542	0.611	1.16	0.0635 (0.0250)	1.25	32.11 (29.22)	0.670	1005 2012	Freon PCA GN <sub>2</sub>
0.182	0.543	0.600	1.21	0.0607 (0.0239)	1.23	30.91 (28.13)	0.664	1005 2012	Freon PCA NTO MON-1
0.155	0.542	0.547	1.15	0.0584 (0.0230)	1.19	29.20 (26.57)	0.627	1005 2012	Freon PCA NTO MON-1

PRECEDING PAGE BLANK NOT FILMED

QUALITY

3 ORIGINAL PAGE IS FOLDOUT FRAME OF POOR QUALITY

Table 10.

Specimen Identification Type	Width w, cm (in.)	Thickness t, cm (in.)	Area A cm <sup>2</sup> (in. <sup>2</sup> )	Sustained Load f <sub>1</sub> , kN (lbf)	Sustained Stress σ <sub>1</sub> , MPa (ksi)	Initial Crack Depth a <sub>1</sub> , cm (in.)	Ini La c
AFSD-11-P	2.8522 (1.1229)	0.1207 (0.0475)	0.3439 (0.0533)	21.93 (4931)	637.86 (92.51)	0.0582 (0.0229)	
AFSD-12-P	2.8545 (1.1238)	0.1219 (0.0480)	0.3477 (0.0539)	22.19 (4989)	638.82 (92.56)	0.0566 (0.0223)	
AFSD-13-P	2.8456 (1.1203)	0.1176 (0.0463)	0.3348 (0.0519)	24.31 (5465)	726.04 (105.30)	0.0716 (0.0282)	
AFSD-14-P	2.8509 (1.1224)	0.1222 (0.0481)	0.3477 (0.0539)	22.19 (4989)	638.20 (92.56)	0.0673 (0.0265)	
AFSD-11-C	2.8486 (1.1215)	0.1224 (0.0482)	0.3484 (0.0540)	25.20 (5665)	723.35 (104.91)	0.0602 (0.0237)	
AFSD-12-C	2.8509 (1.1224)	0.1209 (0.0476)	0.3445 (0.0534)	22.10 (4969)	641.58 (93.05)	0.0561 (0.0221)	
AFSD-13-C	2.8575 (1.1250)	0.1209 (0.0475)	0.3445 (0.0534)	22.10 (4969)	641.58 (93.05)	0.0549 (0.0216)	
AFSD-14-C	2.8540 (1.1236)	0.1209 (0.0476)	0.3452 (0.0535)	22.15 (4979)	641.58 (93.07)	0.0719 (0.0283)	
AFSD-11-H	2.8542 (1.1237)	0.1196 (0.0471)	0.3413 (0.0529)	25.20 (5665)	738.39 (107.09)	0.0556 (0.0219)	
AFSD-12-H	2.8560 (1.1244)	0.1212 (0.0477)	0.3458 (0.0536)	22.10 (4969)	639.24 (92.71)	0.0493 (0.0194)	
AFSD-13-H	2.8512 (1.1225)	0.1222 (0.0481)	0.3484 (0.0540)	22.10 (4969)	634.48 (92.02)	0.0683 (0.0269)	
AFSD-14-H	2.8474 (1.1210)	0.1209 (0.0476)	0.3439 (0.0533)	22.15 (4979)	644.13 (93.42)	0.0648 (0.0255)	

<sup>a</sup>Value of K<sub>Ic</sub> obtained from Table 7.

ORIGINAL PAGE IS  
OF POOR QUALITY

FOLDOUT FRAME

Table 10. Maximum Sustained-Load Flaw-Growth Test Data for AFSD Specimens

Crack Depth $a_1$ , (in.)	Initial Crack Length $2c_1$ , cm (in.)	Final Crack Depth $a_f$ , cm (in.)	Final Crack Length $2c_f$ , cm (in.)	Flaw Growth $a_f - a_1$ , cm (in.)	$\frac{a_1}{2c_1}$	$\frac{\sigma_1}{\sigma_{YS}}$	$\frac{a_1}{t}$	$Q_1$	$\frac{a_1}{Q_1}$ , cm (in.)	M
0582	0.3967	0.0582	0.3967	0	0.147	0.578	0.482	1.13	0.0515	1.
0229)	(0.1562)	(0.0229)	(0.1562)						(0.0203)	
0566	0.3998	0.0566	0.3998	0	0.142	0.579	0.465	1.13	0.0500	1.
0223)	(0.1574)	(0.0223)	(0.1574)						(0.0197)	
0716	0.4227	0.0716	0.4227	0	0.170	0.658	0.609	1.18	0.0610	1.2
0282)	(0.1664)	(0.0282)	(0.1664)						(0.0240)	
0673	0.4072	0.0673	0.4072	0	0.165	0.579	0.551	1.18	0.0574	1.
0265)	(0.1603)	(0.0265)	(0.1603)						(0.0226)	
0602	0.3853	0.0602	0.3853	0	0.156	0.749	0.492	1.15	0.0523	1.
0237)	(0.1517)	(0.0237)	(0.1517)						(0.0206)	
0561	0.3881	0.0561	0.3881	0	0.145	0.665	0.464	1.05	0.0533	1.
0221)	(0.1528)	(0.0221)	(0.1528)						(0.0210)	
0549	0.3940	0.0549	0.3940	0	0.139	0.665	0.455	1.09	0.0503	1.1
0216)	(0.1551)	(0.0216)	(0.1551)						(0.0198)	
0719	0.4605	0.0719	0.4605	0	0.156	0.665	0.595	1.13	0.0635	1.2
0283)	(0.1813)	(0.0283)	(0.1813)						(0.0250)	
0556	0.3810	0.0556	0.3810	0	0.146	0.765	0.465	1.07	0.0518	1.1
0219)	(0.1500)	(0.0219)	(0.1500)						(0.0204)	
0493	0.3894	0.0493	0.3894	0	0.127	0.662	0.407	1.07	0.0460	1.1
0194)	(0.1533)	(0.0194)	(0.1533)						(0.0181)	
0683	0.4161	0.0683	0.4161	0	0.164	0.657	0.559	1.15	0.0597	1.2
0269)	(0.1638)	(0.0269)	(0.1638)						(0.0235)	
0648	0.4249	0.0648	0.4249	0	0.152	0.667	0.536	1.13	0.0577	1.1
0255)	(0.1673)	(0.0255)	(0.1673)						(0.0227)	

ORIGINAL PARTIAL  
OF POOR QUALITY

2 FOLDOUT FRAME

$\frac{\sigma_1}{\sigma_{YS}}$	$\frac{n_1}{t}$	$Q_1$	$\frac{a_1}{Q_1}$ cm (in.)	$M_{K1}$	$K_{TI}$ MPa $\sqrt{m}$ (ksi $\sqrt{in.}$ )	$\frac{K_{TI}}{K_{Ic}}$	Duration of Test, h	Exposure Environment
0.578	0.482	1.13	0.0515 (0.0203)	1.16	32.60 (29.66)	0.662	3020	Air
0.579	0.465	1.13	0.0500 (0.0197)	1.14	31.76 (28.90)	0.645	1004 2016	Freon PCA NTO MON-1
0.658	0.609	1.18	0.0610 (0.0240)	1.25	43.55 (39.63)	0.884	1004 2016	Freon PCA NTO MON-1
0.579	0.551	1.18	0.0574 (0.0226)	1.19	35.44 (32.25)	0.720	1004 2016	Freon PCA NTO MON-1
0.749	0.492	1.15	0.0523 (0.0206)	1.15	37.11 (33.77)	0.790	1004 2016	Freon PCA NTO MON-1
0.665	0.464	1.05	0.0533 (0.0210)	1.14	32.98 (30.01)	0.702	1004 2016	Freon PCA NTO MON-1
0.665	0.455	1.09	0.0503 (0.0198)	1.14	31.91 (29.04)	0.679	1004 2016	Freon PCA NTO MON-1
0.665	0.595	1.13	0.0635 (0.0250)	1.24	39.14 (35.61)	0.833	3020	Air
0.765	0.465	1.07	0.0518 (0.0204)	1.14	37.39 (34.02)	0.803	1004 2016	Freon PCA NTO MON-1
0.662	0.407	1.07	0.0460 (0.0181)	1.11	29.64 (26.97)	0.637	1004 2016	Freon PCA NTO MON-1
0.657	0.559	1.15	0.0597 (0.0235)	1.20	36.27 (33.00)	0.779	1004 2016	Freon PCA NTO MON-1
0.667	0.536	1.13	0.0577 (0.0227)	1.18	35.62 (32.41)	0.765	3020	Air

ORIGINAL PART IS  
OF POOR QUALITY

3 FOLDOUT FRAME

3000 hours of testing. Nine of the twelve specimens, including the three controls, were targeted for a maximum stress-intensity ratio of 0.70; three specimens, one of each type, were targeted for around 0.80, which was the reported threshold stress intensity with exposure to NTO (Ref. 10). The actual experimental stress-intensity ratios range from 0.637 to 0.884. However, none of the twelve specimens showed any evidence of stress-corrosion crack-growth even at the highest stress intensity, which exceeds the reported threshold levels.

#### D. DIMPLING

Backface dimpling occurs in surface-flawed specimens under high tensile stress when the material ligament remaining below the bottom of the flaw (crack) undergoes plastic deformation inward without rupturing. This produces a dimple-like depression on the side of the specimen opposite to the surface flaw. Dimpling was witnessed in all the room-temperature inert fracture testing of AFSD specimens, most of them occurring just before ultimate failure. They were also observed during posttest examination of all the specimens removed from the nominal sustained-load test. A typical example of dimpling is shown in Fig. 19. It was believed that the backface dimples in this instance were produced during the simulated proof-test cycle, when all specimens were subjected to a tensile stress of 690 MPa (100 ksi) for 5 minutes. To confirm this, all proof-test cycles performed on the last test series, the maximum sustained-load testing, were made in air without the propellant cups installed. Load cells and a recorder were installed on two of the static testing machines to measure the loads at which the dimples were formed. The following is a summary of the results from these dimpling tests:

Table 11. AFSD Specimen Backface Dimple Stresses

Type of Specimen	Minimum Stress, MPa (ksi)	Maximum Stress, MPa (ksi)	Average Stress, MPa (ksi)
Parent Metal	489 (70.9)	652 (94.6)	572 (82.8)
Center Weld	275 (39.4)	323 (46.8)	296 (42.9)
Heat-Affected	290 (42.1)	321 (46.6)	304 (44.1)

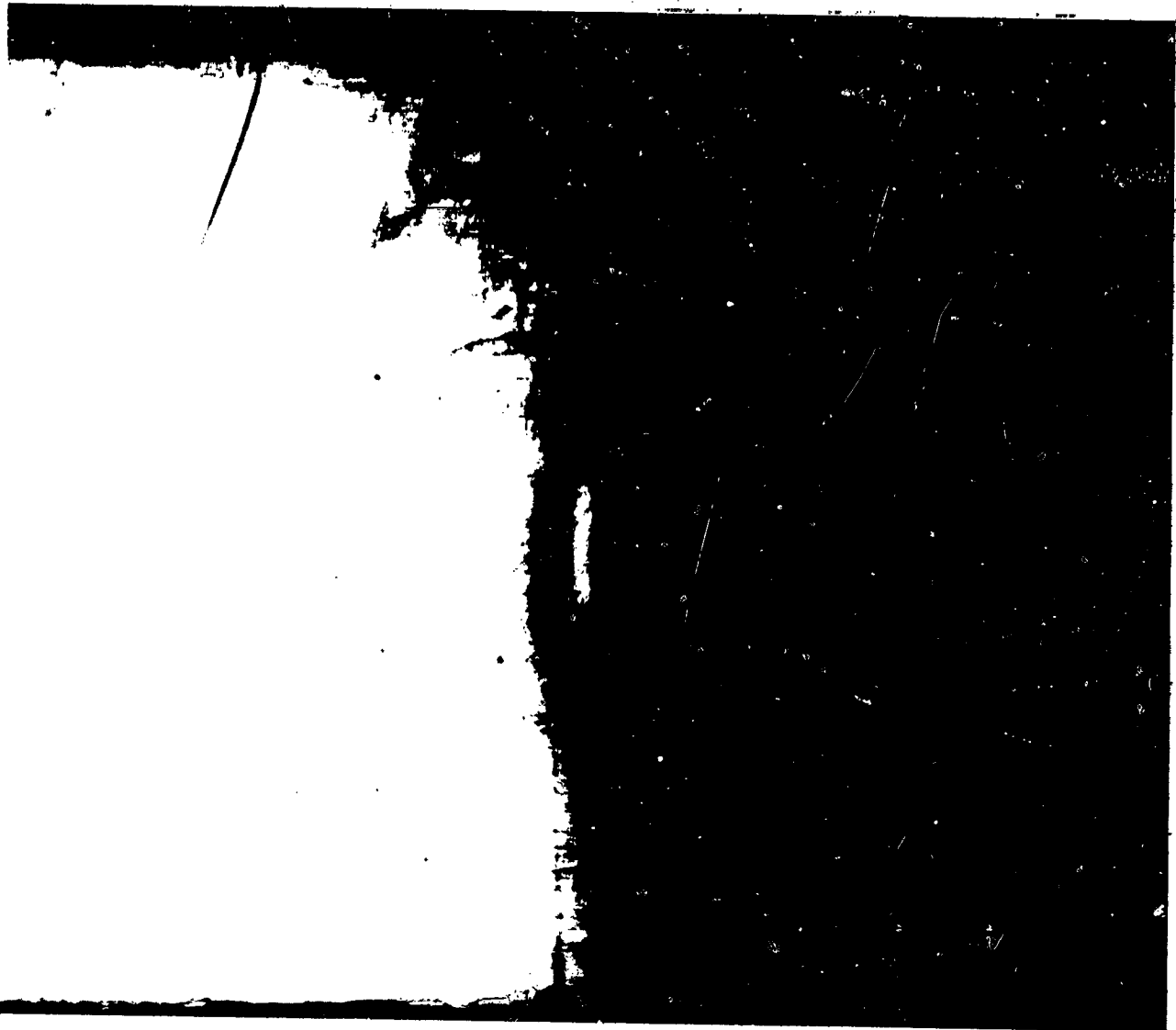


Figure 19. Typical Example of Posttest Backface Dimple from Sustained-Load Testing

#### E. SCANNING ELECTRON MICROSCOPY

Scanning electron photomicrographs of typical AFSD test specimens exposed to Freon PCA, NTO MON-1,  $\text{GN}_2$ , and air are shown in Figures 20 to 24. The zone of sustained load testing, which lies between the boundaries of precracking and posttest marking, are visible and identified in each of these figures. None of the SEM fractographs taken of all test specimens show any stress-corrosion crack growth between the initial fatigue crack and the posttest marking. Some of the specimens exhibited lateral fracturing that occurred in the plastically-yielded ligament below the surface flaw (deep-dimple zone) during posttest marking. In these instances, the cyclic tensile stress was higher than required for marking. High-magnification photomicrographs of cross sections taken of these lateral fractures (fractographs) have shown that they are definitely not the results of stress-corrosion cracking. A fractograph of specimen AFSD-5-C is shown in Fig. 25.



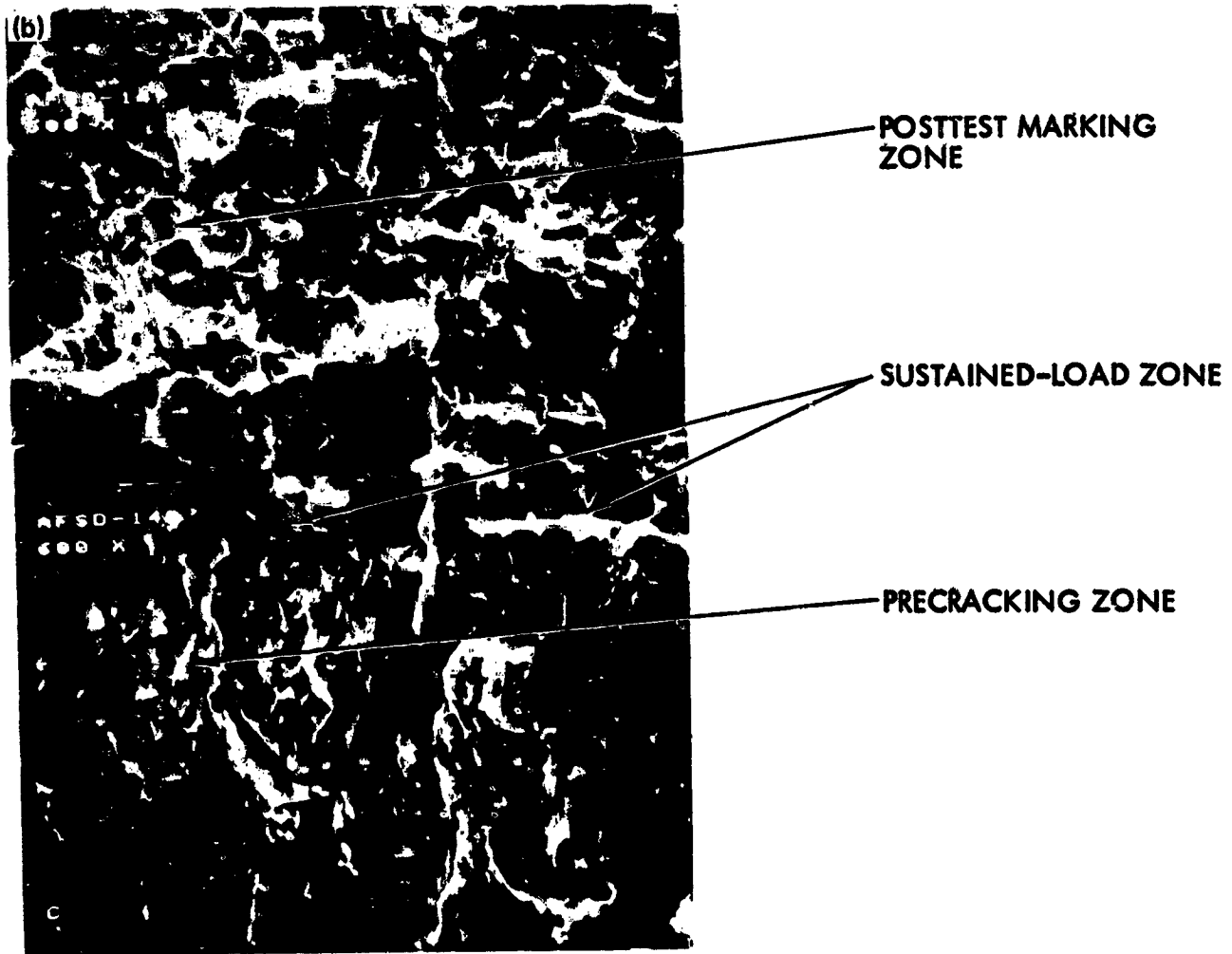


Figure 20. Parent-Metal Specimen AFSD-14-P After Sustained-Load-Testing Exposure to Freon PCA and NTO MON-1: (a) 43x; (b) 600x

ORIGINAL PAGE IS  
OF POOR QUALITY

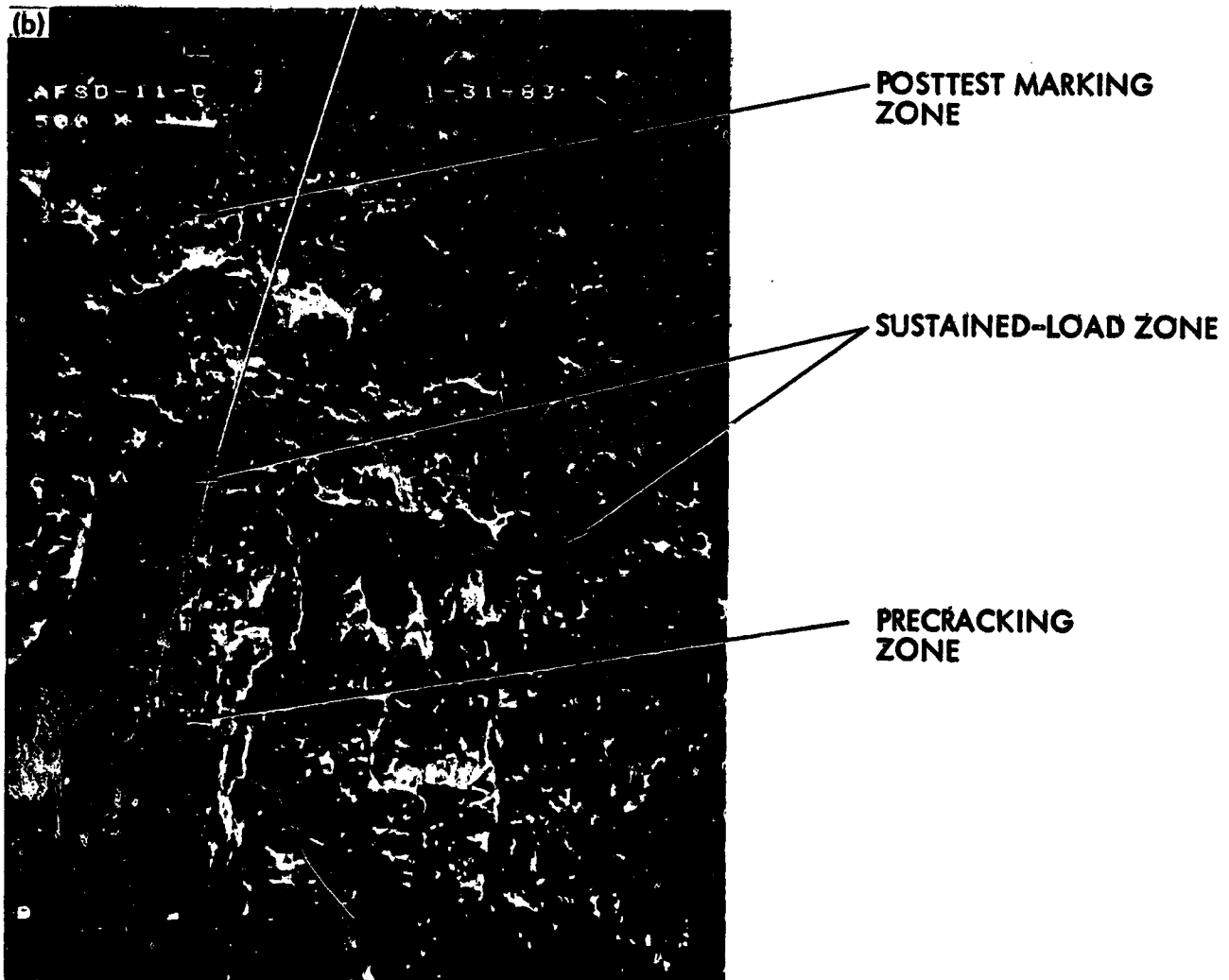
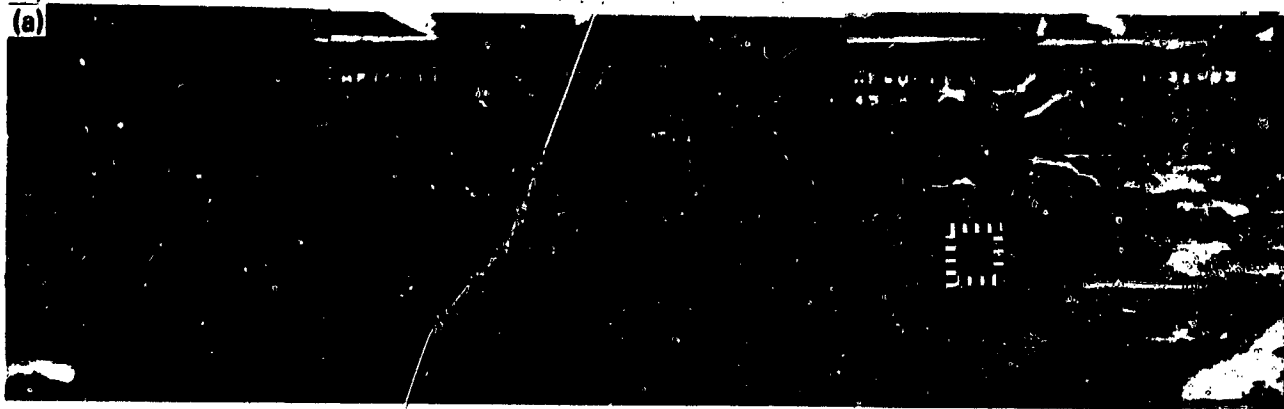
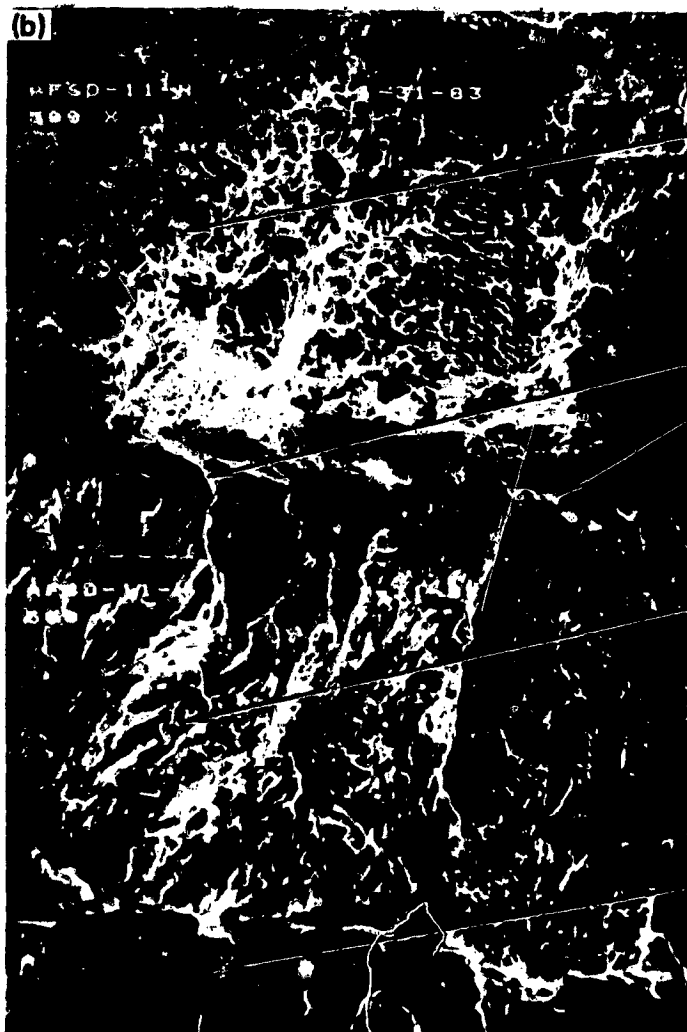
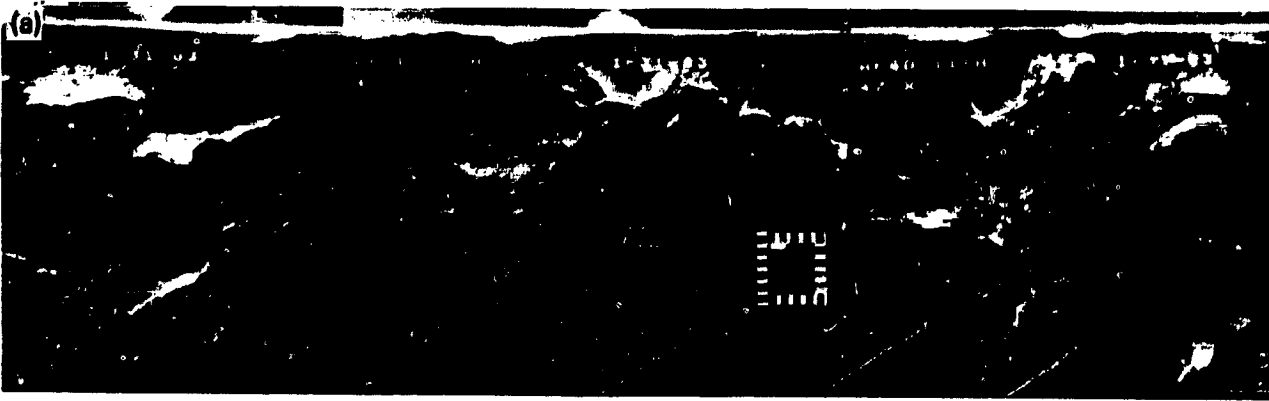


Figure 21. Center-Weld Specimen AFSD-11-C After Sustained-Load-Testing Exposure to Freon PCA and NTO MON-1: (a) 45x; (b) 500x

ORIGINAL PAGE IS  
OF POOR QUALITY



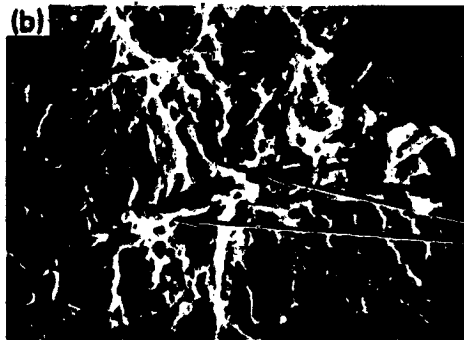
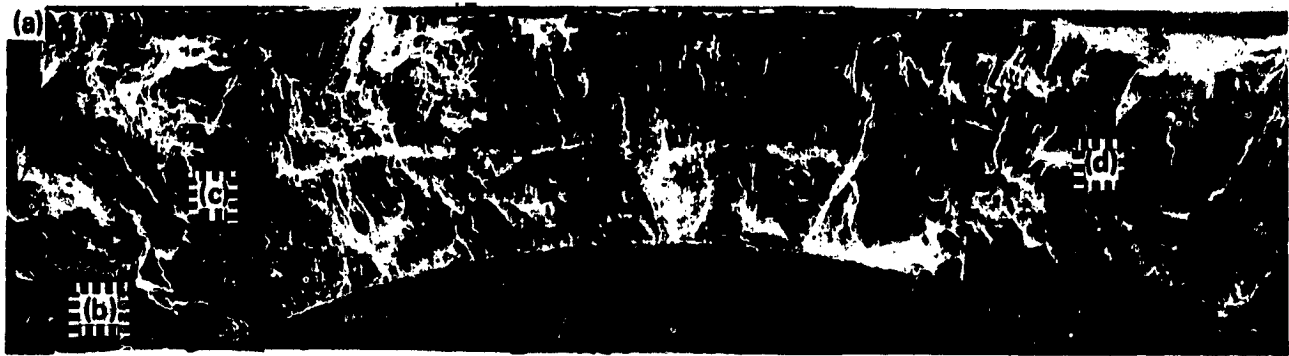
POSTTEST MARKING  
ZONE

SUSTAINED-LOAD ZONE

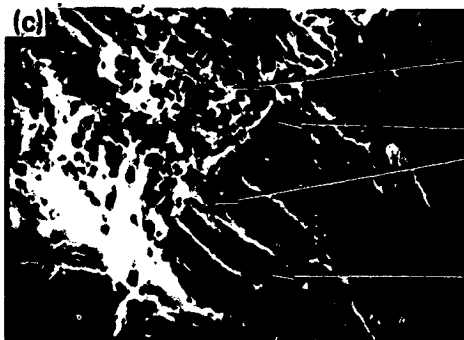
PRECRACKING  
ZONE

STARTER  
NOTCH

Figure 22. Weld-Heat-Affected-Zone Specimen AFSD-11-H After Sustained-Load-Testing Exposure to Freon PCA and NTO MON-1: (a) 47x; (b) 500x

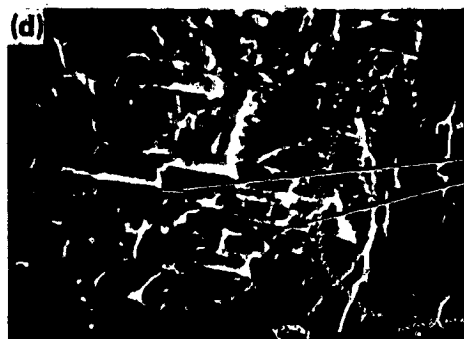


LATERAL  
FRACTURES



POSTTEST  
MARKING  
ZONE  
SUSTAINED-LOAD  
ZONE

PRECRACKING  
ZONE



LATERAL  
FRACTURES

Figure 23. Control Specimen AFSD-4-H After Sustained-Load-Testing Exposure to Freon PCA and  $\text{GN}_2$ : (a) 60 $\times$ ; (b), (c), and (d) 1000 $\times$

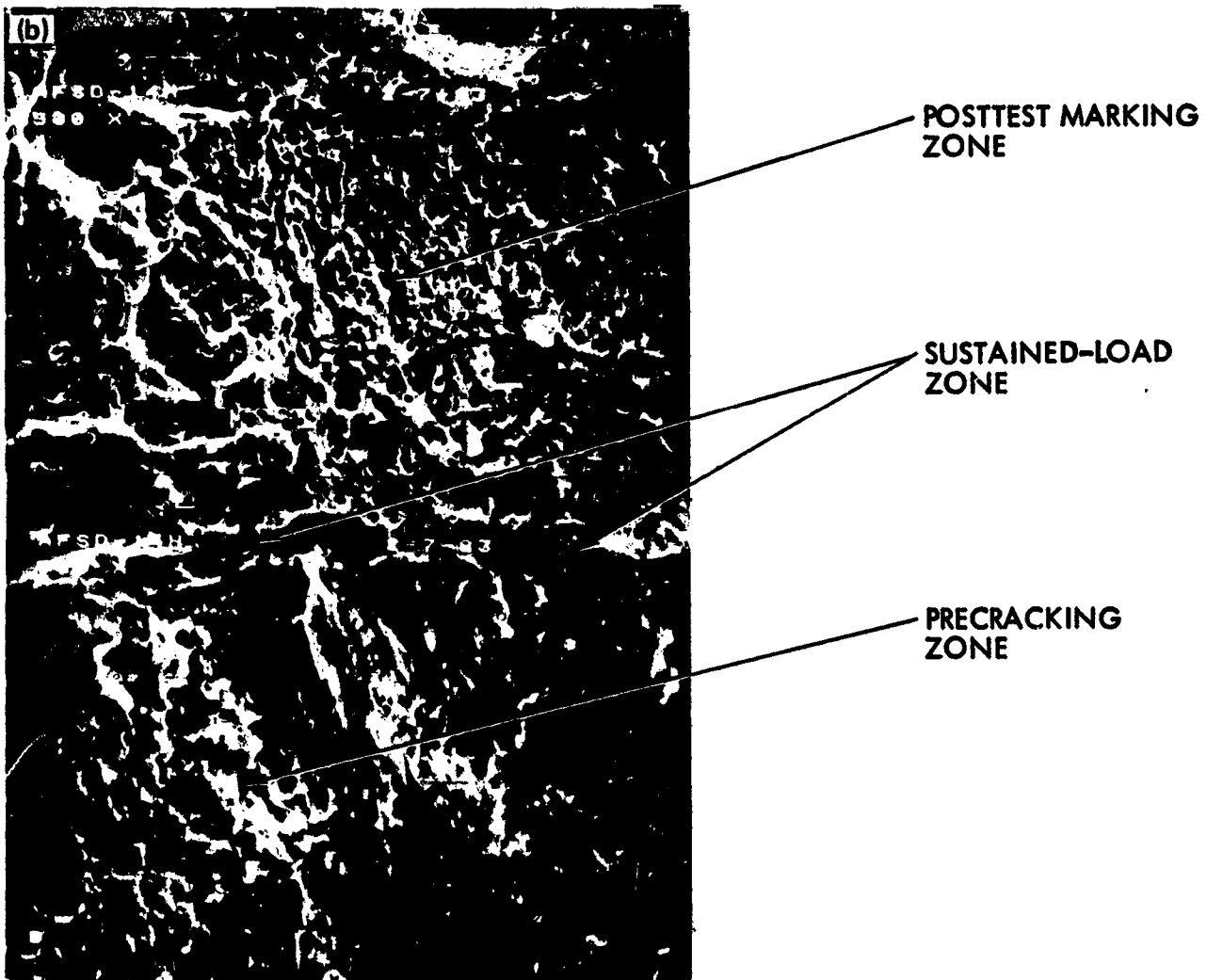


Figure 24. Control Specimen AFSD-14-H After Sustained-Load-Testing  
Exposure to Air Only: (a) 50x; (b) 500x

ORIGINAL PAGE IS  
OF POOR QUALITY

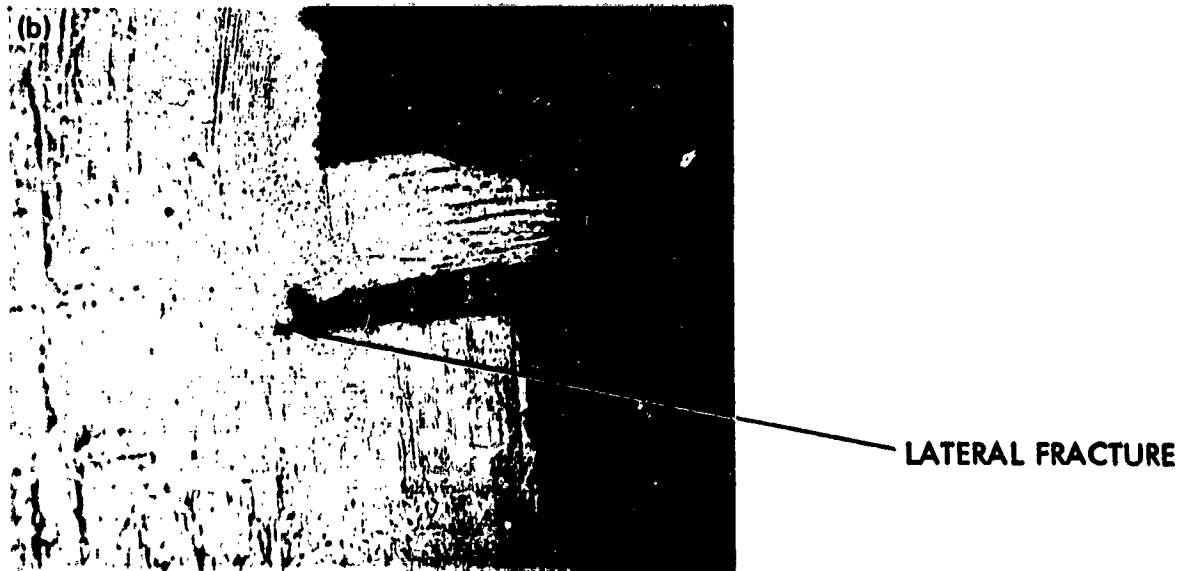
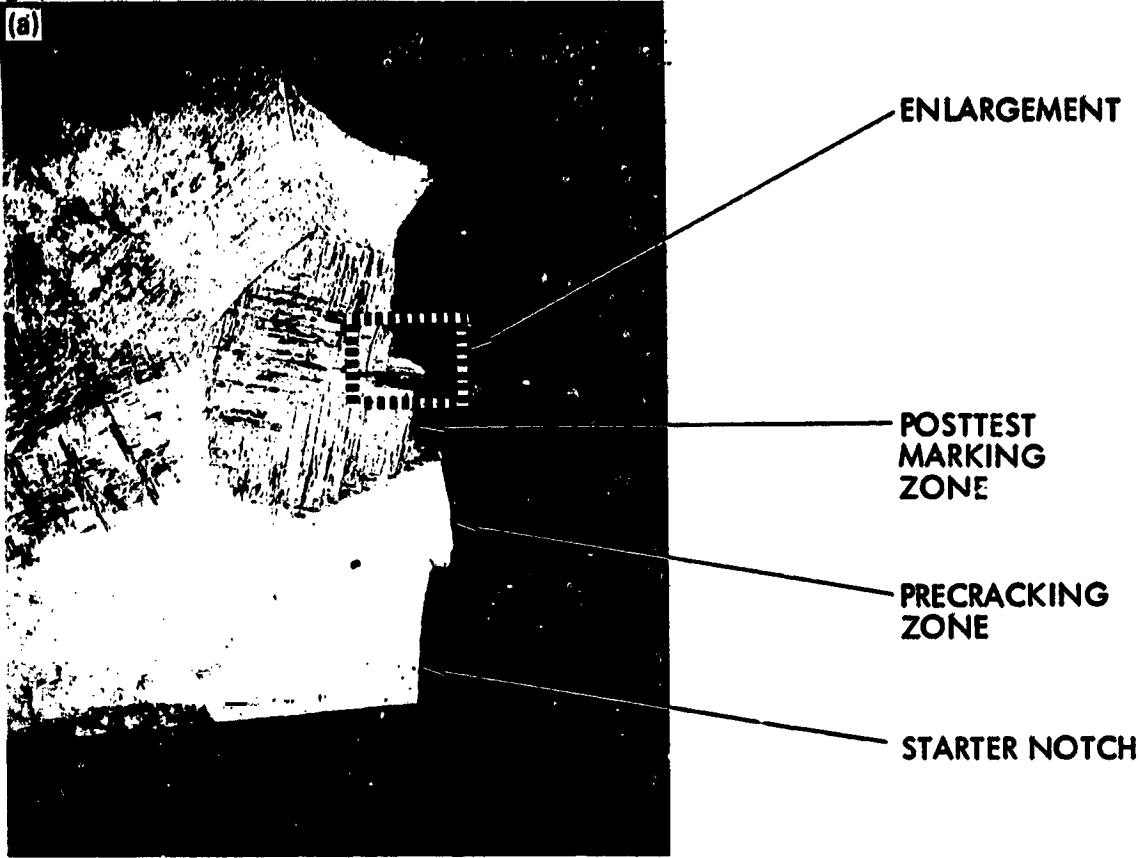


Figure 25. Cross Section of Lateral Fracture in Backface Dimple of AFSD-5-C Specimen: (a) 75 $\times$ ; (b) 500 $\times$

## SECTION V

### CONCLUSIONS

The stress-corrosion crack-growth sensitivity of the high-strength, lightweight propellant tank material titanium alloy Ti-6Al-4V has been experimentally evaluated by sustained-load testing with sequential exposure to Freon PCA for 1000 hours and to NTO MON-1 for 2000 hours. The results of these tests are summarized in Tables 8 through 10. Based on these experimental results, the following conclusions have been made:

- (1) Titanium alloy Ti-6Al-4V is not adversely affected in a sustained-stress environment when exposed to Freon PCA at stress-intensity ratios up to 0.80; therefore, Freon PCA is a suitable cleaning solvent and refreezing fluid for an NTO MON-1 propellant tank made from this material.
- (2) Titanium alloy Ti-6Al-4V is not adversely affected in a sustained-stress environment when exposed to NTO MON-1 at stress-intensity ratios up to 0.80; therefore, the alloy is a suitable lightweight, high-strength tank material for this oxidizer propellant.
- (3) The sequential exposure of titanium alloy Ti-6Al-4V to Freon PCA and NTO MON-1 in a sustained-stress environment does not require a rigorous cleaning procedure to remove all traces of Freon PCA before the introduction of NTO MON-1 to prevent stress-corrosion crack growth at stress-intensity ratios up to 0.80.
- (4) Although this test data for titanium alloy Ti-6Al-4V is limited to one heat, one heat treatment, and one size and thickness of test specimen, it does include parent-metal, center-of-weld, and weld-heat-affected-zone types of specimens and covers a broad range of stress-intensity ratios from 0.593 to 0.884. Therefore, the results of this fracture mechanics testing is expected to be applicable to other Ti-6Al-4V propellant tanks of similar design for other spacecraft or missile applications.

**SECTION VI**  
**RECOMMENDATIONS**

The use of Freon PCA as a cleaning solvent and referee fluid can be recommended for the manufacturing and acceptance testing of NTO MON-1 propellant tanks made of titanium alloy Ti-6Al-4V. To this extent, the following additional recommendations are made:

- (1) Cleaning procedure to remove Freon PCA from the tanks before the introduction of NTO MON-1 can be limited to a gaseous nitrogen (GN<sub>2</sub>) purge to remove the liquid, a short vacuum purge (nominally 5 minutes) to remove vapors, followed by a back filling with GN<sub>2</sub> or GHe to exclude ambient air.
- (2) If, because of structural limitations, a vacuum purge cannot be used, a warm GN<sub>2</sub> purge at temperatures around 49°C to 66°C (120°F to 150°F) for approximately 30 minutes or longer, depending on the complexity of the propellant tank system, should remove most of the Freon PCA vapors.

NOTE: If trace quantities of Freon PCA remain in the tank, there will be no adverse chemical reaction that will induce stress-corrosion cracking when the tank is serviced with NTO MON-1 and pressurized to the designed operating condition.

When the present MIL-SPEC NTO MON-1 is supplemented with a purified grade of NTO, it is recommended that additional fracture-mechanics tests be made to determine the stress-corrosion crack-growth sensitivity of titanium alloy Ti-6Al-4V, or other propellant tank materials, to the new purified NTO oxidizer.



DEFINITION OF TERMS

Term or Symbol	Definition or Identification
a	crack depth of the semielliptical surface flaw, cm (in.) (2.54 cm = 1 in.)
A	cross-sectional area of test specimen, cm <sup>2</sup> (in. <sup>2</sup> ) (6.452 cm <sup>2</sup> = 1 in. <sup>2</sup> )
C	center-of-weld specimen
2c	crack length of the semielliptical surface flaw, cm (in.)
f	uniaxial tensile load, kN (lbf) (4.448 kN = 1,000 lbf)
flaw	surface crack including EDM notch and precrack (also post-test mark)
H	weld-heat-affected-zone specimen
K <sub>I</sub>	plane-strain stress-intensity factor,  $\frac{MN}{m} \sqrt{m} \text{ or } MPa \sqrt{m} \quad (\text{ksi } \sqrt{\text{in.}})$ $(1.099 \text{ MPa } \sqrt{m} = 1 \text{ ksi } \sqrt{\text{in.}})$
K <sub>Ic</sub>	critical plane-strain stress-intensity factor,  $MPa \sqrt{m} \quad (\text{ksi } \sqrt{\text{in.}})$
K <sub>Ii</sub>	plane-strain stress-intensity factor at the initial conditions,  $MPa \sqrt{m} \quad (\text{ksi } \sqrt{\text{in.}})$
K <sub>Ie</sub>	experimental critical plane-strain stress-intensity factor or fracture toughness for given material of a specified type, thickness, and flaw size,  $MPa \sqrt{m} \quad (\text{ksi } \sqrt{\text{in.}})$

Term or Symbol	Definition or Identification
mark	zone between sustained-load crack and the posttest fatigue cracking boundary
$M_K$	stress-intensity magnification factor for deep surface flaws
P	parent-metal-type specimen
precrack	zone between EDM notch edge and initial fatigue cracking boundary
Q	surface flaw-shape parameter
t	thickness of test specimen, cm (in.)
w	width of test specimen, cm (in.)
$\sigma$	uniform gross stress applied remote from flaw and perpendicular to the plane of flaw,
	$\frac{MN}{m^2}$ or MPa (ksi)
	(6.895 MPa = 1 ksi)
$\sigma_u$	ultimate tensile strength of material, MPa (ksi)
$\sigma_{ys}$	tensile yield strength of material, MPa (ksi)

Subscripts	Definition or Identification
c	at critical conditions
e	at experimental conditions
f	at final conditions
i	at initial conditions

Abbreviations	Definition or Identification
AFRPL (or RPL)	Air Force Rocket Propulsion Laboratory (United States)
AFSD	Air Force Headquarters Space Division (United States)
ASTM	American Society for Testing and Materials
EB	electron beam
EDM	electric-discharge machine
ETS	Edwards Test Station (JPL)
HAC	Hughes Aircraft Company
IPA	isopropyl alcohol
JPL	Jet Propulsion Laboratory (California Institute of Technology)
MMH	monomethylhydrazine
MON	mixed oxides of nitrogen
NTO	nitrogen tetroxide
PCA	precision cleaning agent
SEM	scanning electron microscope
TIG	tungsten-inert-gas weld
TMCA	Titanium Metals Corporation of America
UTS	ultimate tensile strength
YS	yield strength

## REFERENCES

1. Anthony, J. K., and Butcher, W. W., "Propulsion Subsystem for the Satellite Data Systems Satellite," in Proceedings of the JANNAF Propulsion Meeting, Volume V, CPIA Publication 315, Marc' 1980.
2. "NASA Pre-Alert: Test Specimen, Metallic 6Al-4V Titanium Immersed in Hydrazine, and Glass-Encapsulation," Alert E4-70-03A. National Aeronautics and Space Administration, Washington, D.C., August 16, 1971.
3. Boyd, W. K., et al., "Stress-Corrosion Cracking in Metals," NASA Space Vehicle Design Criteria, NASA SP-8082. National Aeronautics and Space Administration, Washington, D.C., August 1971.
4. Tiffany, C. F., et al., "Fracture Control of Metallic Pressure Vessels," NASA Space Vehicle Design Criteria (Structures), NASA SP-8040. National Aeronautics and Space Administration, Washington, D.C., May 1970.
5. R. O. Technical Bulletin FST-2, E. I. DuPont DeNemours and Co. (Inc.), "Freon" Products Division, Wilmington, Delaware, June 1979.
6. USAF Propellant Handbook Nitric Acid/Nitrogen Tetroxide Oxidizers, Volume II, AFRPL-TR-76-76. Martin Marietta Corporation, Denver, Colorado, February 1977.
7. "Fracture Mechanics Test Specimens," Drawing No. 10091560, Revision A, Sheets 1 and 2. Jet Propulsion Laboratory, Pasadena, California, June 6, 1979 (JPL internal document).
8. Toth, L. R., and Moran, C. M., Nitrogen Tetroxide Impurities Study. JPL 715-42 or AFRPL-TR-80-36, Jet Propulsion Laboratory, Pasadena, California, April 1980 (JPL internal document).
9. Bjorklund, R. A., Stress-Corrosion Crack-Growth Study of Titanium Alloy Ti-15V-3Al-3Cr-3Sn Exposed to Nitrogen Tetroxide MON-1 or Monomethylhydrazine. JPL D-1 or AFRPL-TR-82-053, Jet Propulsion Laboratory, Pasadena, California, June 1982.
10. Tiffany, C. F., and Masters, J. N., Investigation of Flaw Growth Characteristics of 6Al-4V Titanium Used in Apollo Spacecraft Pressure Vessels, NASA CR-65586. National Aeronautics and Space Administration, Washington, D.C., 1967.
11. Masters, J. N., "Cyclic and Sustained Flaw Growth Characteristics of 6Al-4V Titanium," NASA CR-92231. National Aeronautics and Space Administration, Washington, D.C., 1968.

APPENDIX A

LINEAR-ELASTIC FRACTURE MECHANICS

This appendix presents the linear-elastic fracture-mechanics expressions used to calculate the fracture toughness of the specific material, specimen type, and thickness, with one nominal flaw size, from the experimentally derived data. The derivation and development of these expressions by Inglis, Irwin, Tiffany, Masters, Kobayashi, and Smith are summarized in Ref. 3.

The general equation that describes the relationship between a part-through surface flaw and the applied remote gross stress is

$$K_I = 1.1 \sqrt{\pi} (a/Q) M_K \sigma \quad (A-1)$$

The flaw shape parameter  $Q$  is obtained from Fig. A-1. The magnification factor  $M_K$  is obtained from Fig. A-2. For calculation of the initial sustained-load plane-strain stress-intensity factor for a given environment, Eq. (A-1) becomes

$$K_{Ii} = 1.1 \sqrt{\pi} (a/Q)_i M_{Ki} \sigma_i \quad (A-2)$$

The experimental critical plane-strain stress-intensity factor is calculated by substituting the experimental critical data obtained from the inert fracture tests into Eq. (A-1); i.e.,

$$K_{Ie} = 1.1 \sqrt{\pi} (a/Q)_e M_{Ke} \sigma_e \quad (A-3)$$

The stress-intensity ratio  $K_{Ii}/K_{Ie}$  is calculated for each specimen because it represents the severity of stress the specimen was subjected to during the sustained-load test for stress-corrosion crack growth.

The critical plane-strain stress-intensity factor,  $K_{Ic}$ , for a specific material, specimen type, and thickness, and at a given environmental condition must be obtained from laboratory tests involving a variety of flaw sizes (i.e.,  $a$  and  $2c$  dimensions). In addition to surface-flawed specimens, these tests could include fatigue-cracked bend specimens, crack-line loaded specimens, center-cracked and edge-cracked sheet specimens, and fatigue-cracked round notched-bar specimens.

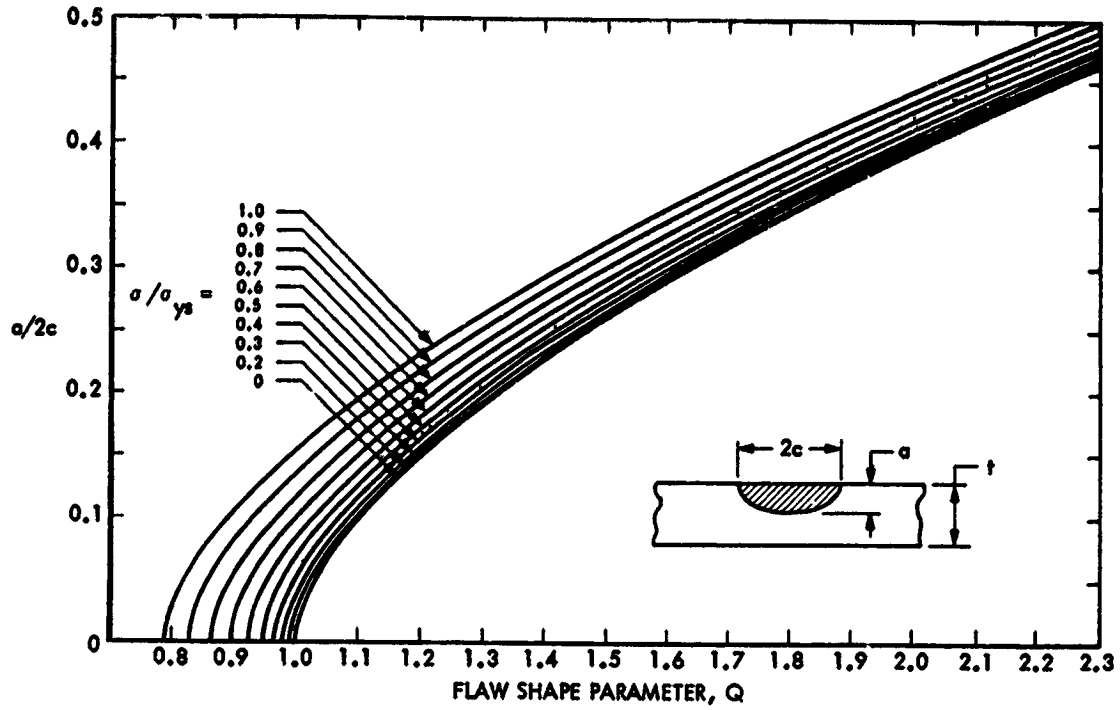


Figure A-1. Shape Parameter Curves for Surface Flaws

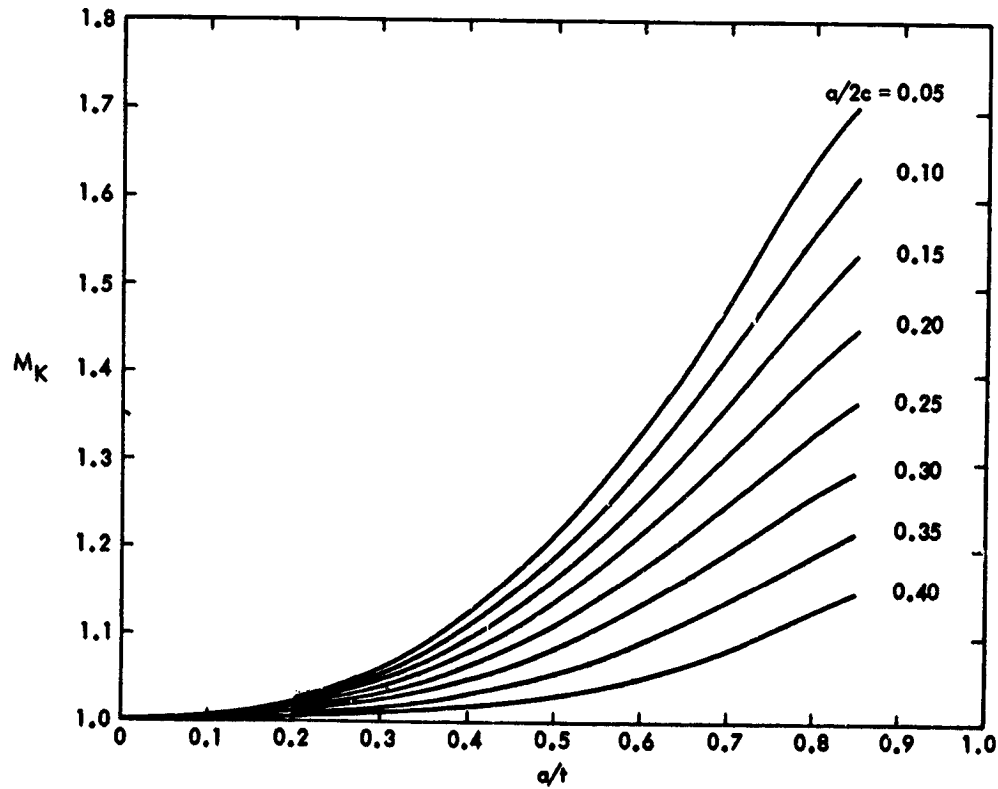


Figure A-2. Magnification Factor Curves